Reciprocating Internal Combustion Engines

Prof. Rolf D. Reitz
Engine Research Center
University of Wisconsin-Madison

2014 Princeton-CEFRC
Summer School on Combustion
Course Length: 15 hrs

(Mon.- Fri., June 23 – 27, 2014)

Short course outine:

Engine fundamentals and performance metrics, computer modeling supported by in-depth understanding of fundamental engine processes and detailed experiments in engine design optimization.

Day 1 (Engine fundamentals)
- Part 1: IC Engine Review, 0, 1 and 3-D modeling
- Part 2: Turbochargers, Engine Performance Metrics

Day 2 (Combustion Modeling)
- Part 3: Chemical Kinetics, HCCI & SI Combustion
- Part 4: Heat transfer, NOx and Soot Emissions

Day 3 (Spray Modeling)
- Part 5: Atomization, Drop Breakup/Coalescence
- Part 6: Drop Drag/Wall Impinge/Vaporization/Sprays

Day 4 (Engine Optimization)
- Part 7: Diesel combustion and SI knock modeling
- Part 8: Optimization and Low Temperature Combustion

Day 5 (Applications and the Future)
- Part 9: Fuels, After-treatment and Controls
- Part 10: Vehicle Applications, Future of IC Engines

Beale, 1999

ERC Spray modeling

Blob injection model

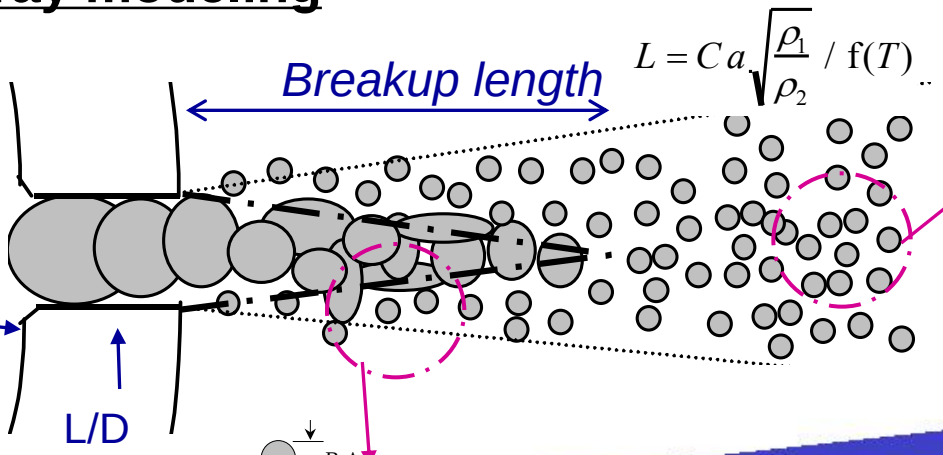

RT Model

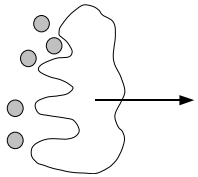

Kelvin-Helmoltz
Rayleigh Taylor
Linearized instability analysis

KH Model

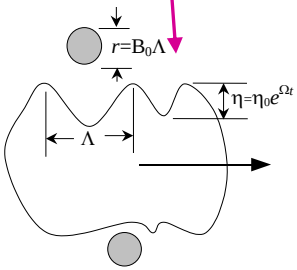

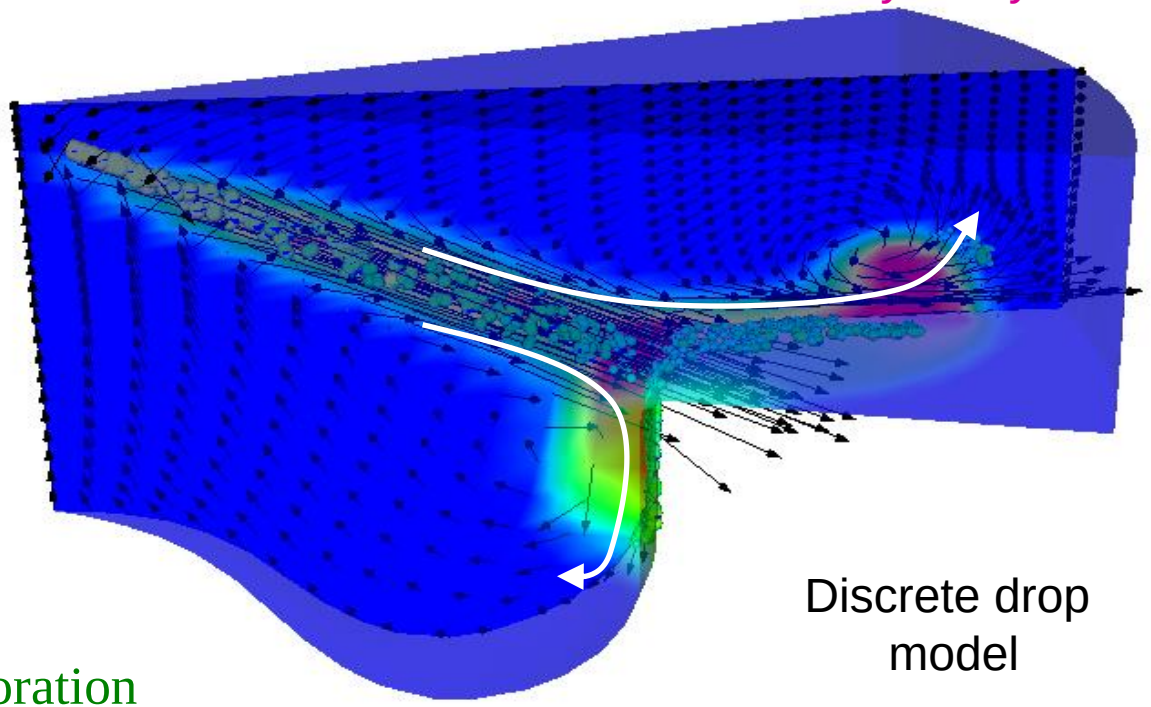

Discrete drop model

Spray Models

Nozzle flow/cavitation
Jet atomization
Drop breakup } KH-RT
Drop collision/coalescence
Drop drag
Multi-component fuel evaporation
Spray-wall impingement

Liu, 1993

Droplet drag modeling

Steady-state Stokes viscous drag, added-mass and Basset history integral

$$\mathrm{dv/dt} = \quad \mathbf{F} = 6\pi r \mu_g \mathbf{v} + \tfrac{1}{2}(\tfrac{4}{3}\pi r^3 \rho_g)\frac{d\mathbf{v}}{dt} + 6r^2\sqrt{\pi\mu\rho_g}\int_0^t \frac{d\mathbf{v}/dt'}{\sqrt{t-t'}}dt'$$

General form

$$\boxed{\rho_L V_d \, d\mathbf{v}/\,dt = C_D A_f \frac{\rho_g U^2}{2}\{\mathbf{U}/|\mathbf{U}|\}}$$

$$C_d = \begin{cases} 24\,\mathrm{Re}_d^{-1}(1+\mathrm{Re}_d^{2/3}/6), & \mathrm{Re}_d < 1000 \\ 0.424, & \mathrm{Re}_d \geq 1000 \end{cases}$$

- Drop distortion (TAB model)

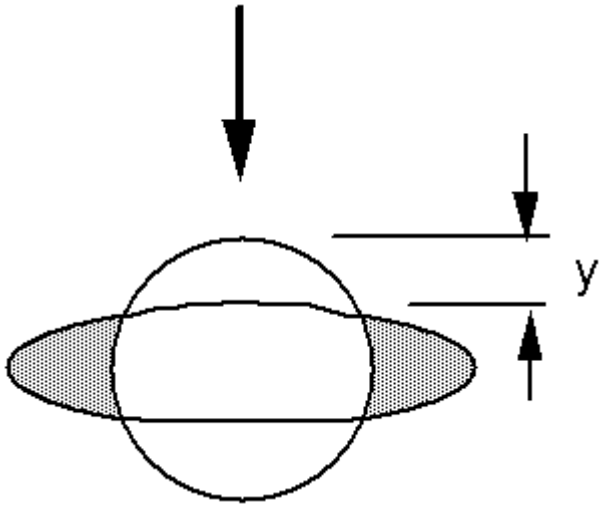

$$\ddot{y} = -5\frac{\mu_l}{\rho_l}\frac{\dot{y}}{r_d^2} - \frac{8\sigma y}{\rho_l r_d^3} + \frac{2}{3}\frac{\rho}{\rho_l}\frac{U_{rel}^2}{r_d^2}$$

$$C_d = C_{d,sphere}(1+2.632y)$$

Gosman, 1981

Turbulence & drop dispersion

- Monte Carlo method

$$\mathbf{u} = \bar{\mathbf{u}} + \mathbf{u}'$$

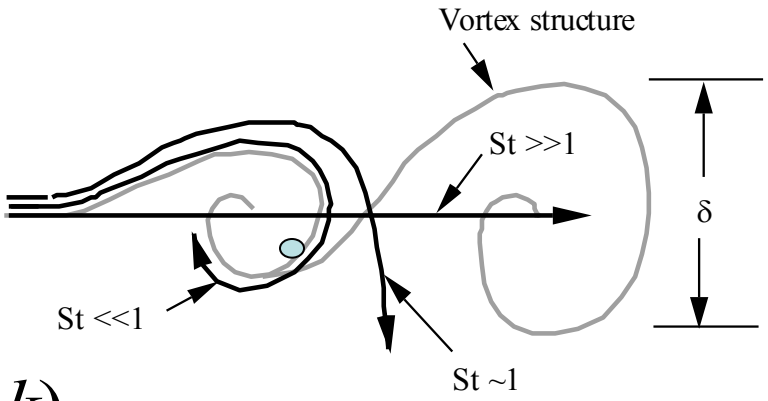

$$G(\mathbf{u}') = (4/3\pi k)^{-3/2} \exp(-3|\mathbf{u}'|^2/4k)$$

Stokes #
$St = t_e/t_p$

Drop-eddy interaction time

Eddy life time

$$t_e = l/\sqrt{2k/3}$$

$$l = C_\mu^{3/4} k^{3/2}/\varepsilon$$

Residence time

$$t_p = l/|\bar{\mathbf{u}} - \mathbf{v}|$$

$$\delta = l$$

$$t_{\text{int}} = \min(t_e, t_p)$$

Wachters, 1966

Spray wall impingement

At low approach velocities (We) drops rebound elastically

With hot walls cushion of vapor fuel forms under the drop

As approach velocity is increased, normal velocity component decreases and drop may break up

Beyond We = 40 liquid spreads into surface layer

At high temperatures film boiling takes place

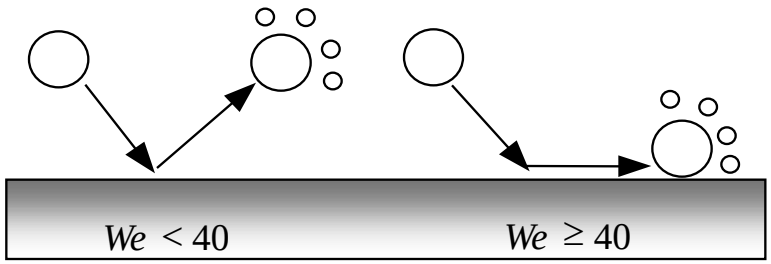

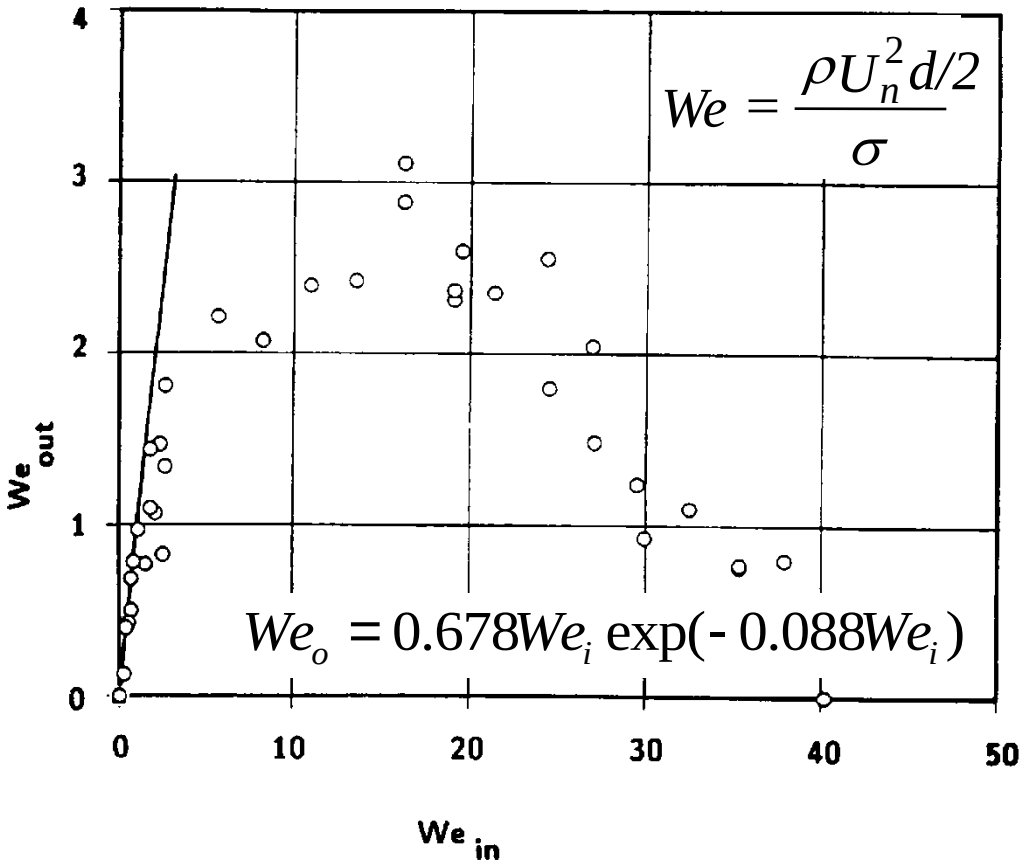

Naber, 1988

Dry wall impingement models

Stick - drops stick to the wall

Reflect - drops rebound

Slide/Jet - incident drop leaves tangent to the surface

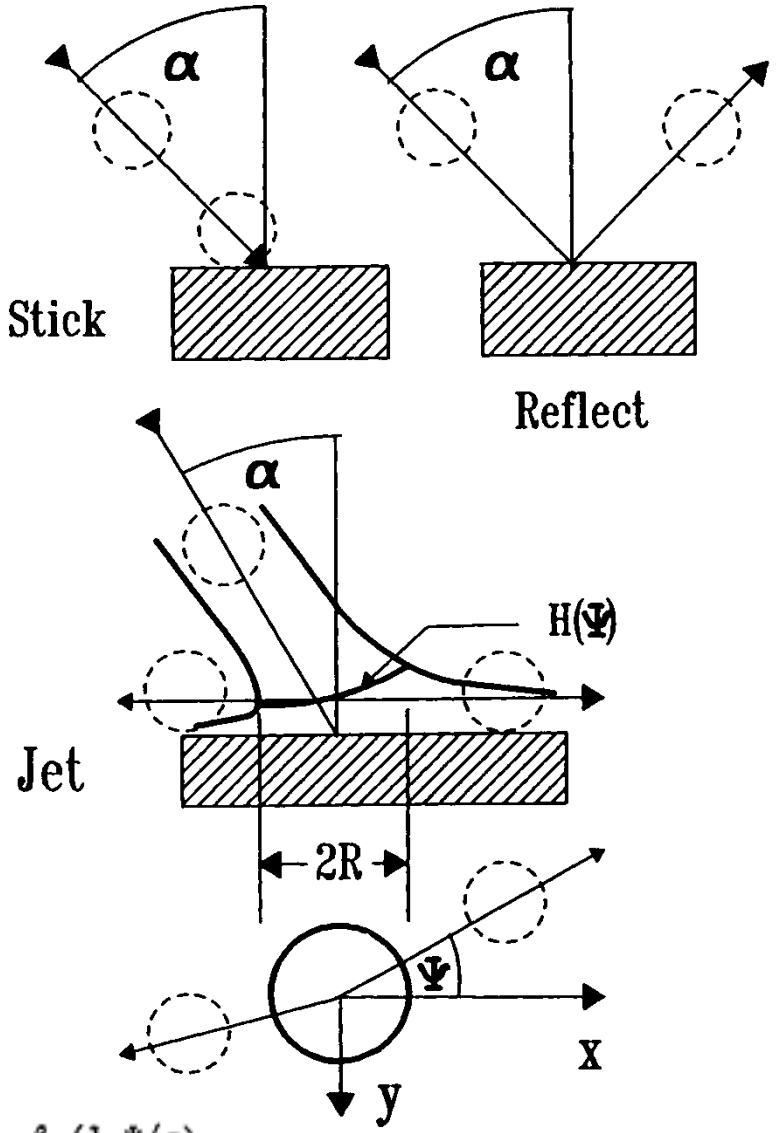

From mass and momentum conservation:

$$\psi = -\frac{\pi}{\beta}\ln\{1 - p(1-\exp(-\beta)\}$$

where $0 < p < 1$ random number

$$\sin\alpha = \left(\frac{\exp(\beta)+1}{\exp(\beta)-1}\right) / 1 + (\pi/\beta)^2$$

$$H(\Psi) = H_{\pi} e^{\beta\,(1-\Psi/\pi)}$$

Senecal, 1997
Lippert, 2000

ERC wall impingement models

- Rebound or slide based on We
- Enhanced breakup due to drop destabilization $B_1 = 1.73$

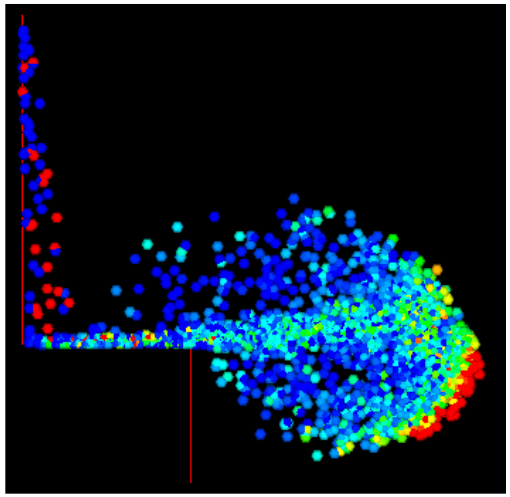

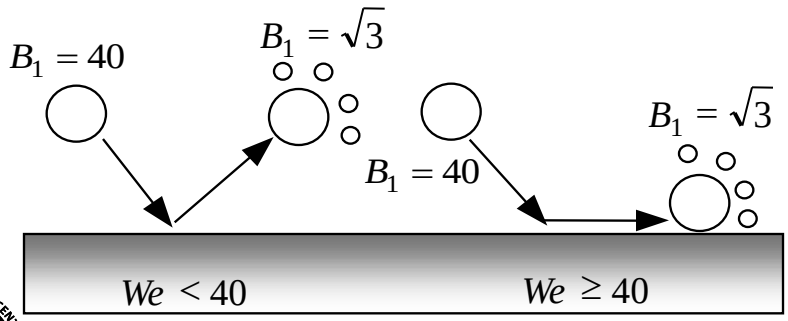

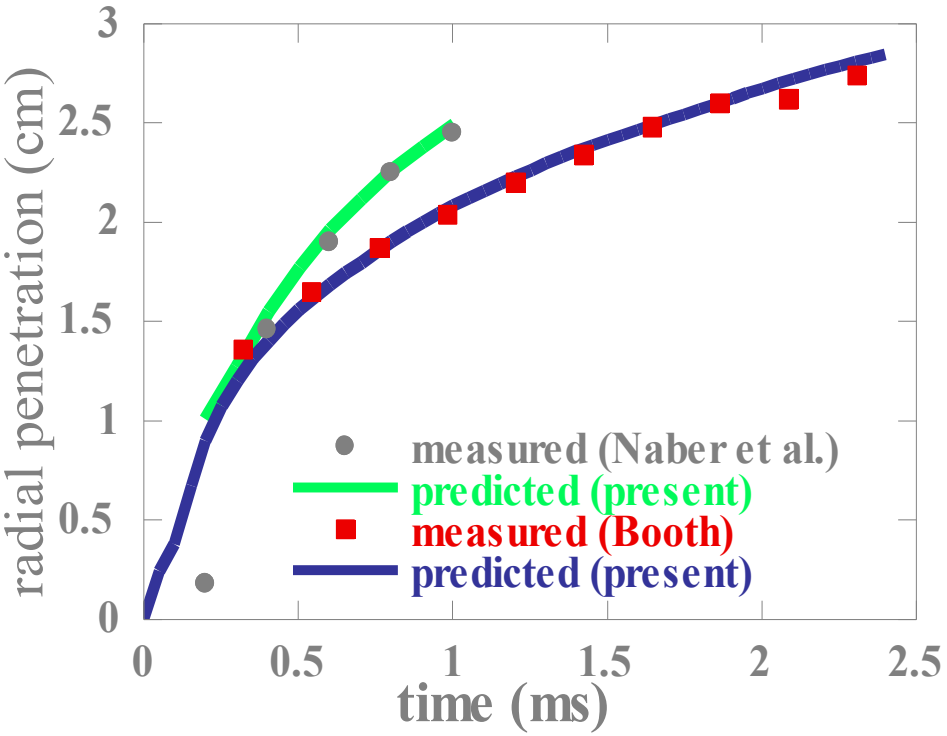

Wet wall impingement – grid independent model

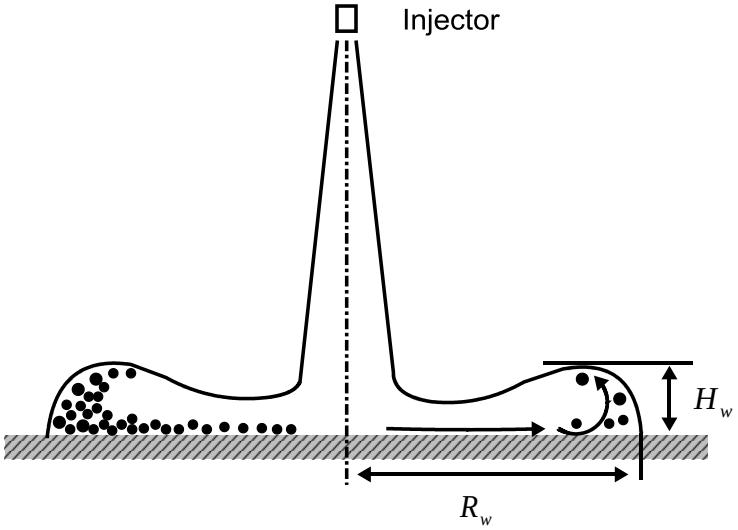

Saffman lift force on splashed drops

$$\rho_L V_d \, d\mathbf{v}/dt = C_D A_f \frac{\rho_g U^2}{2} \{\mathbf{U}/|\mathbf{U}|\} + F_{Saff}$$

$$F_{Saff} = 1.61 \mu_g d \, |\mathbf{U}\text{-}\mathbf{v}| \sqrt{\mathrm{Re}_g}$$

$$\mathrm{Re}_g = \frac{\rho_g}{\mu_g} d^2 \left| \frac{du}{dy} \right|$$

Drop splash criterion

$$E^2 = We_{L,i} \frac{1}{\min(\frac{h_o}{d}, 1) + \frac{1}{\sqrt{\mathrm{Re}_{L,i}}}} > E^2_{crit} = 3,330$$

Splash mass ratio

$$\dot{m} = \left[0.1 + 0.4 \min(\frac{h_o}{d}, 1) \right]^{\left(\frac{C}{We_{L,i}}\right)^{1/4}}$$

$$C = \sqrt{We_{L,inj}} = \sqrt{\frac{\rho_L U_{inj}^2 d_{noz}}{\sigma}}$$

Wall Jet Model

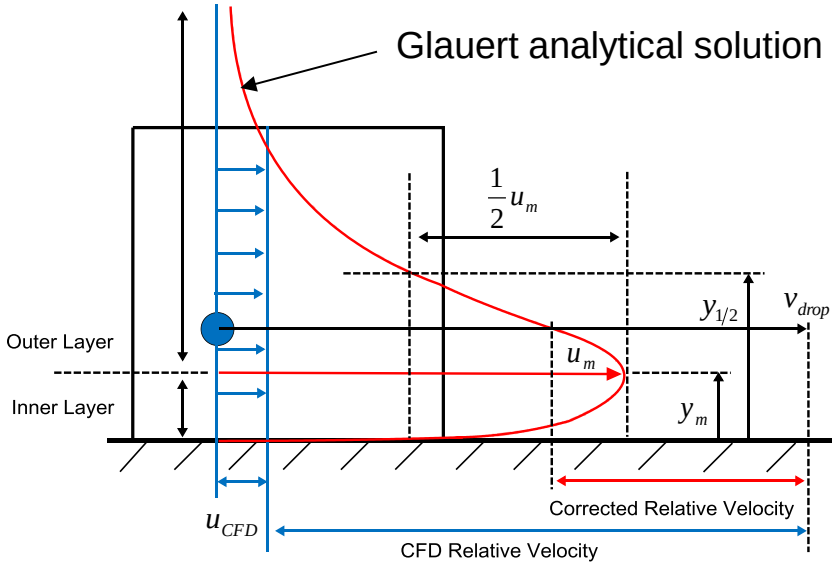

Part 6: Drop Drag/Wall Impinge/Vaporization/Sprays

Deng, 2014

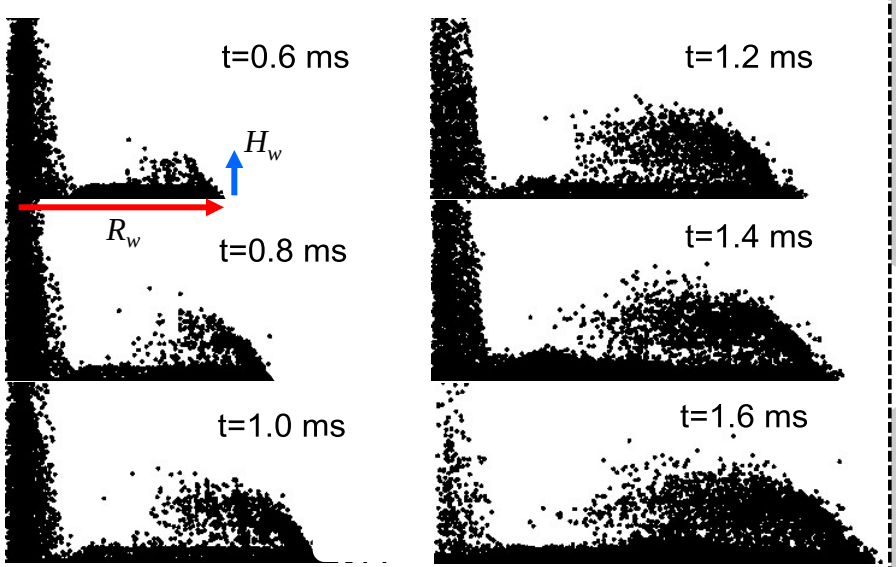

Simulation results

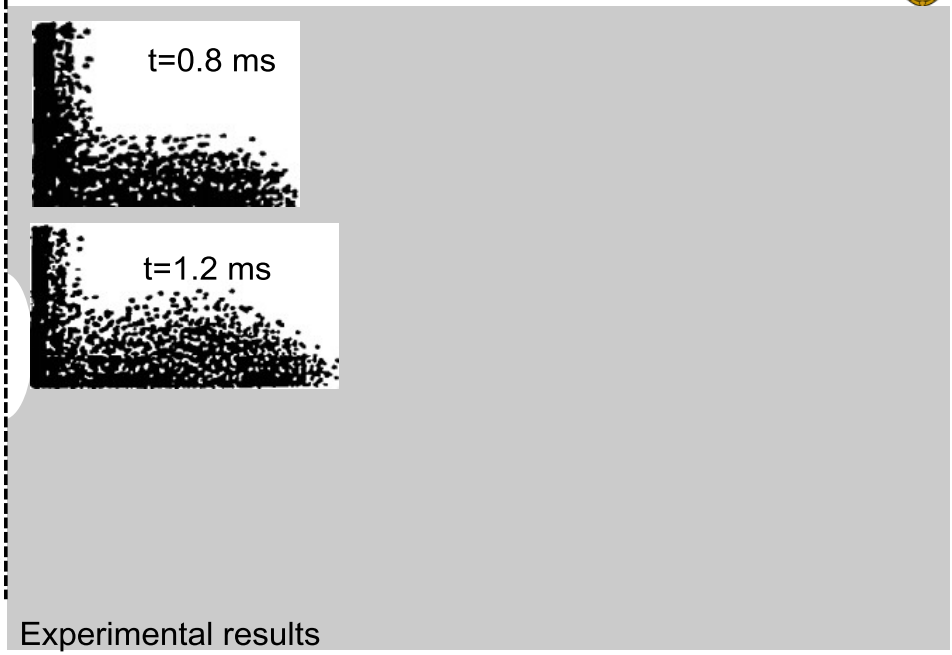

Experimental results

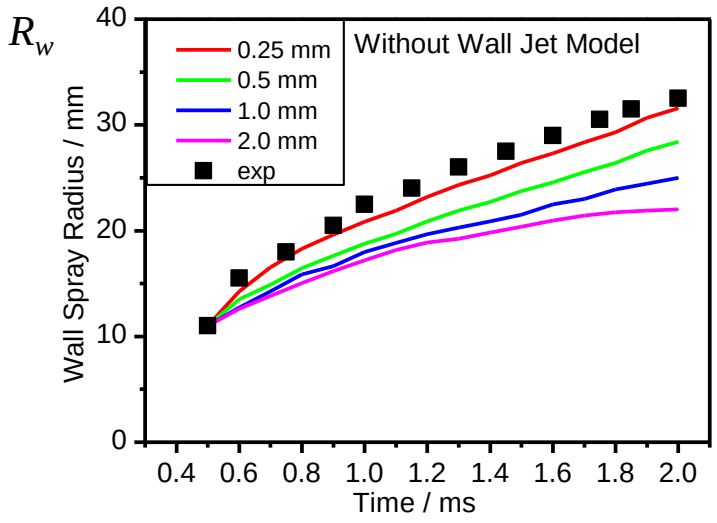

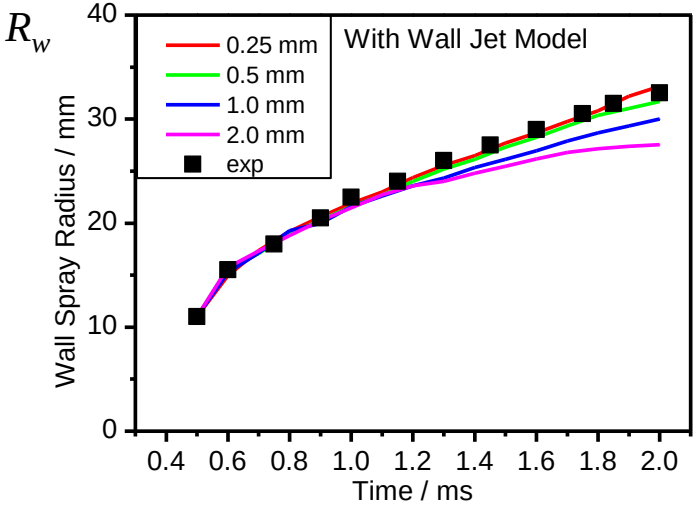

Deng, 2014

Effect of ambient pressure

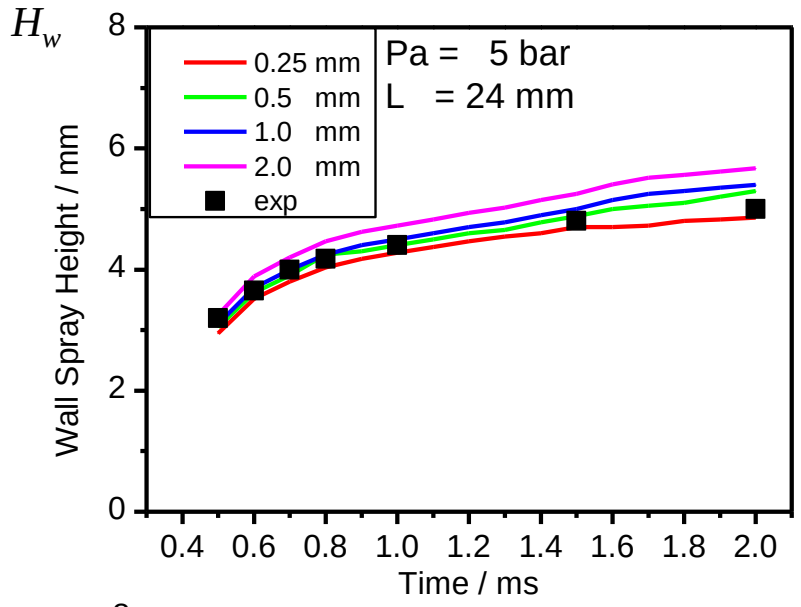

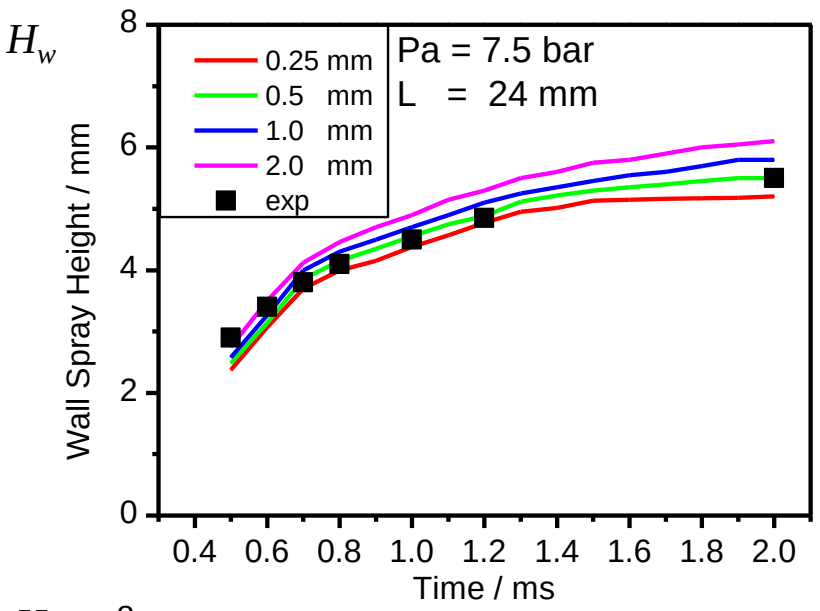

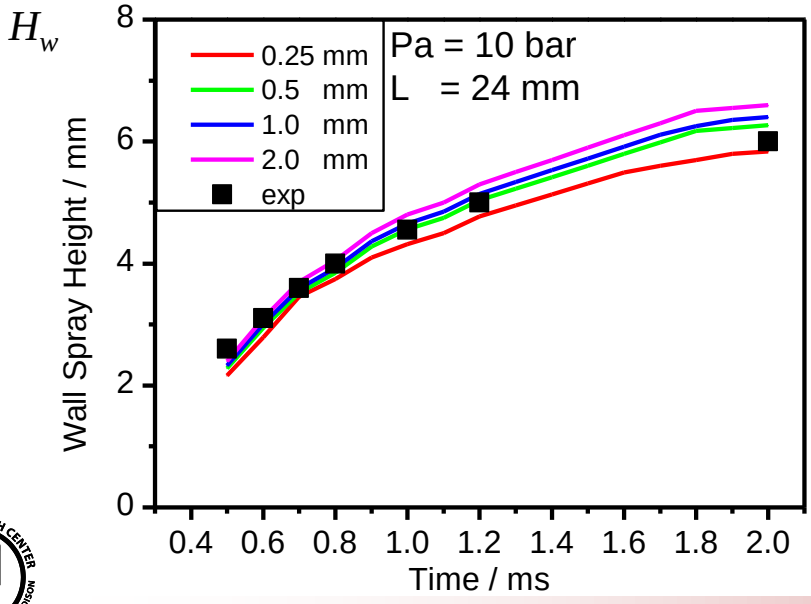

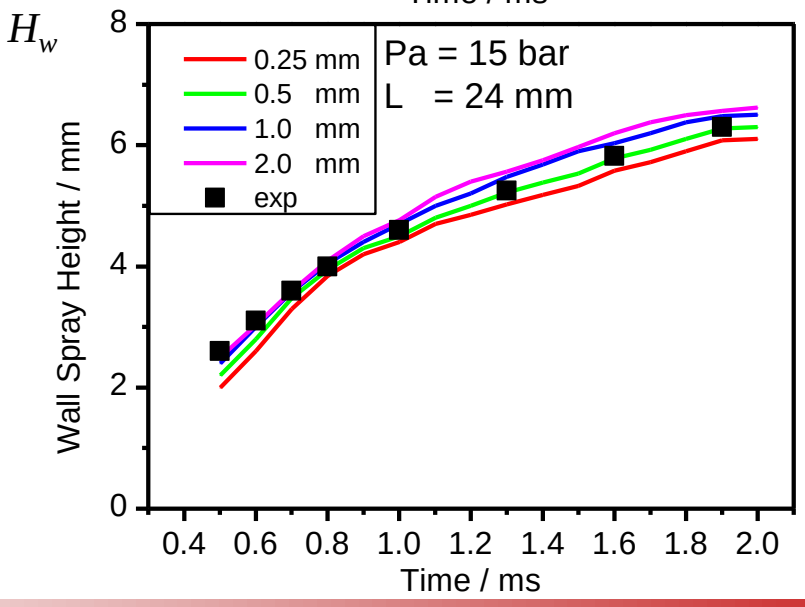

Sirignano, 1999
Law, 1976-77
Aggarwal, 2000

Drop Vaporization

- well understood for single component, low ambient pressure
- D^2 Law

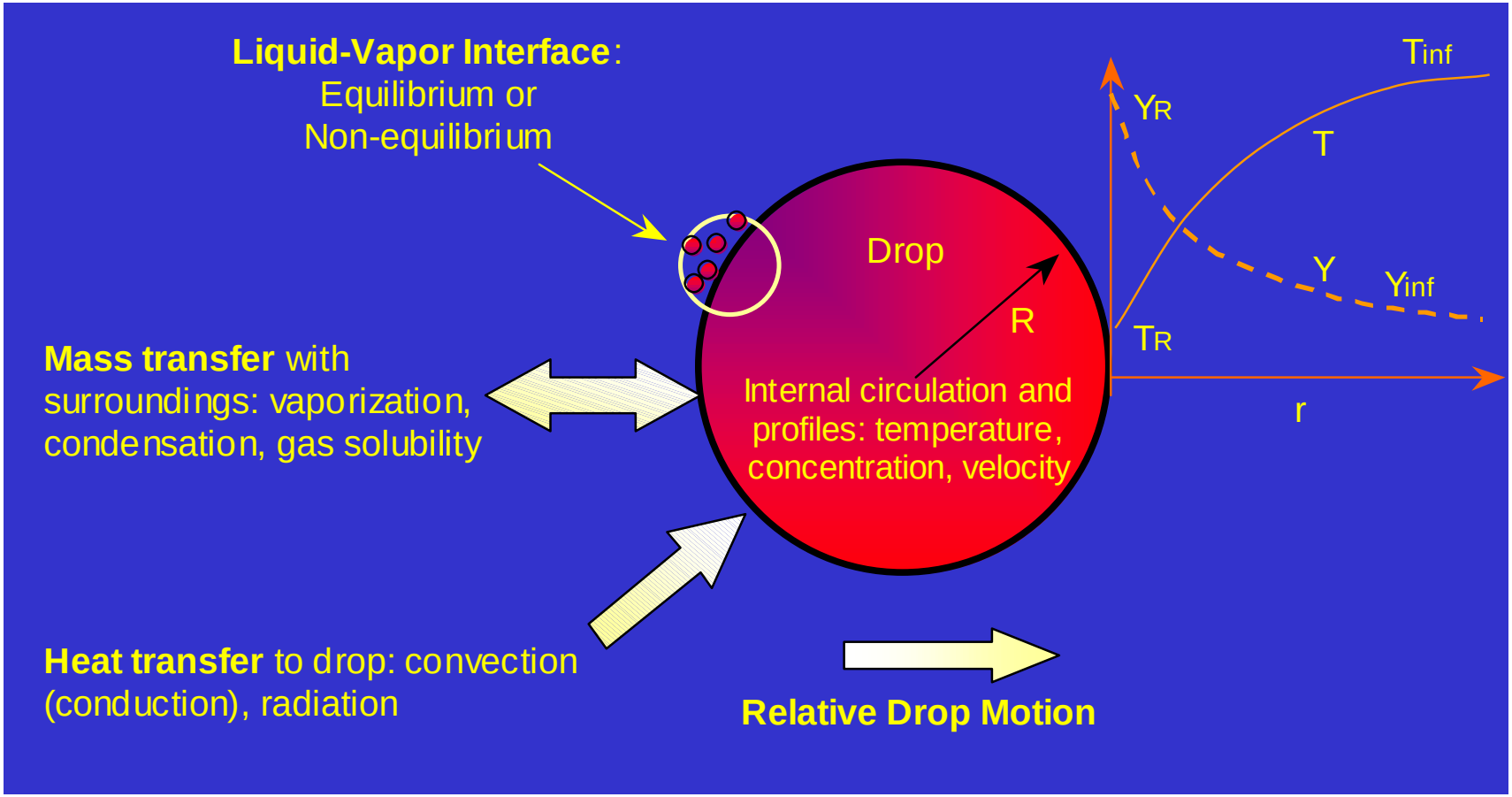

Amsden, 1989
Lefebvre, 1989

KIVA vaporization models

Frossling correlation

$$\mathbf{R} = dr/dt = -\rho DBSh/(2\rho_l r)$$

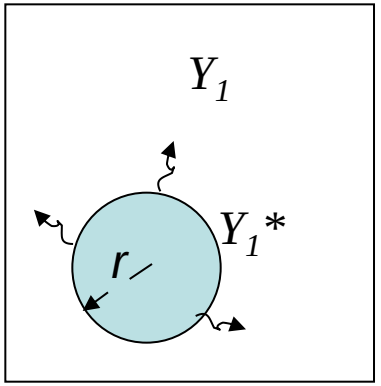

Mass transfer number

$$B = (Y_1^* - Y_1)/(1 - Y_1^*)$$

Sherwood number

$$Sh = (2.0 + 0.6\,\mathrm{Re}_d^{1/2} Sc^{1/3})\frac{\ln(1+B)}{B}$$

Fuel mass fraction at drop surface

$$Y_1^* = W_1 / \{W_1 + W_0(\frac{p}{p_v(T_d)} - 1)\}$$

Vapor pressure P_v from thermodynamic tables

Amsden, 1989
Lefebvre, 1989

Drop heat-up modeling

Change in drop temperature from energy balance

$$\rho_d \frac{4}{3}\pi r^3 c_d \dot{T}_d - 4\pi r^2 RL(T_d) = 4\pi r^2 Q_d$$

Rate of heat conduction to drop from

Ranz-Marshall correlation

$$Q_d = \alpha(T_\infty - T_d)Nu/2\rho r$$

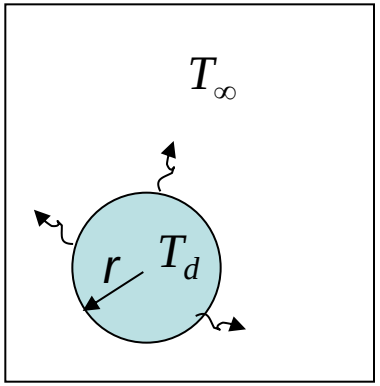

where

$$Nu = (2.0 + 0.6\,\mathrm{Re}_d^{1/2}\,\mathrm{Pr}^{1/3})\frac{\ln(1+B)}{B}$$

Vaporization regimes

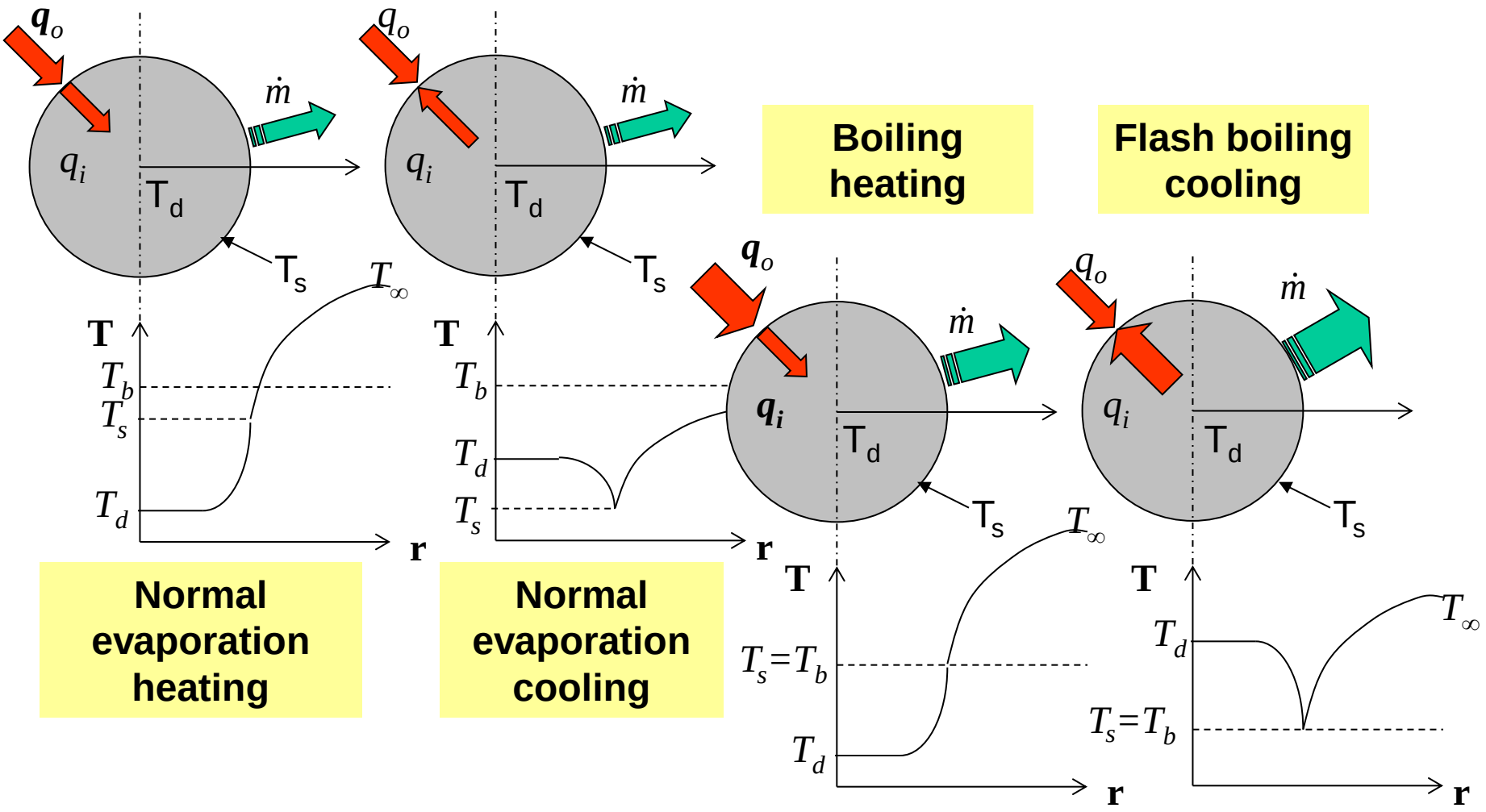

Ra, 2003

Vaporization regimes

Normal evaporation

energy balance

$$\dot{m}L(T_s) = h_{i,eff}(T_d - T_s) + \frac{\kappa \bar{C}_P \dot{m}}{\exp\left[\frac{2r_o \bar{C}_P \dot{m}}{\lambda Nu} - \frac{[C_A](y_{F\infty} - y_{Fs})}{\lambda}\frac{Sh}{Nu}\right] - 1}(T_\infty - T_s)$$

mass balance

$$\dot{m} = g_m \ln(1 + B_M) = g_m \ln\left(1 + \frac{y_{Fs} - y_{F\infty}}{1 - y_{Fs}}\right)$$

$g_m = Sh\,\rho\bar{D}/(2R)$

Boiling evaporation (T_b from Clausius Clapeyron equation)

$$\dot{m}L(T_b) = (h_{i,eff} + \alpha_{sh})(T_d - T_b) + \frac{\kappa \bar{C}_P \dot{m}}{\exp\left[\frac{2r_o \bar{C}_P \dot{m}}{\lambda Nu} - \frac{[C_A](y_{F\infty} - 1)}{\lambda}\frac{Sh}{Nu}\right] - 1}(T_\infty - T_b)$$

$$\Delta T = T_d - T_b$$

Superheated droplet correlation (Adachi et al., 1997)

$$\alpha_{sh} = 0.76\Delta T^{0.26} \quad (0 \le \Delta T < 5)$$
$$= 0.027\Delta T^{2.33} \quad (5 \le \Delta T < 25)$$
$$= 13.8\Delta T^{0.39} \quad (25 \le \Delta T)$$

$$h_{i,eff} = \frac{\lambda}{\delta_e}, \quad \delta_e = \sqrt{\pi \alpha_{eff} t}$$

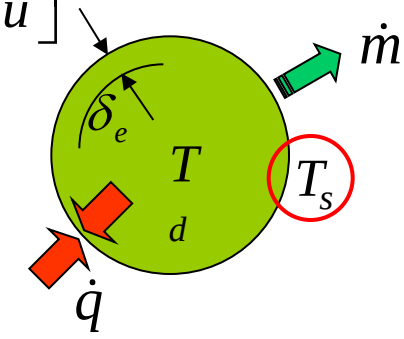

Ra, 2003

Lippert, 1997

Multi-component fuel modeling

Gasoline

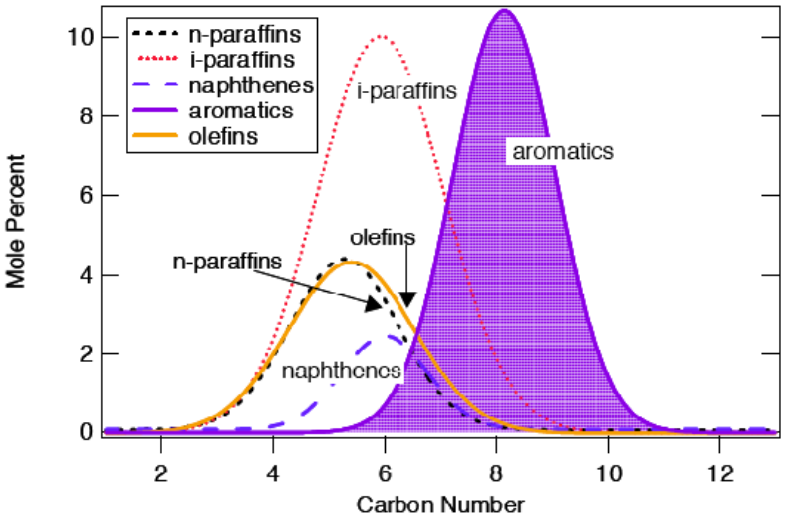

Diesel

	diesel A	diesel B
Aromatic [%]	34	16
Sulfur [ppm]	10.5	7.3
Parafins [%]	33	42
Napthenes [%]	33	42
Olefin [%]	0.2	0.3
Cetane#	~43	~47
C/H ratio	7.014	6.393

Common automotive fuels are multi-component

Components: Various molecular weights and chemical structures

Three approaches;

i) single component approximation

ii) continuous multi-component

iii) discrete multi-component

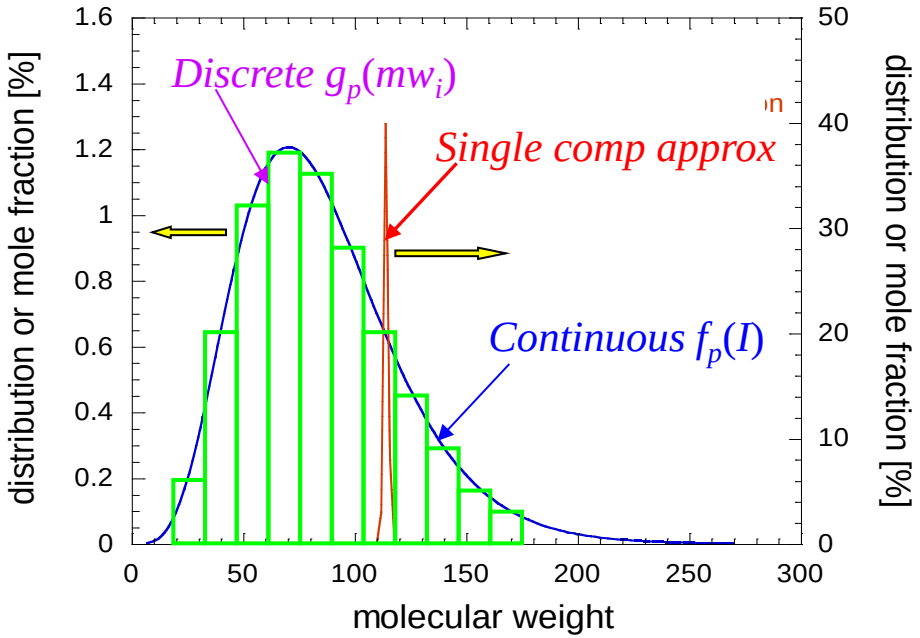

Yi, 2001
Ra, 2003, 2009

Multi-component model formulation

Continuous Multi-Component

- Continuous system of a liquid phase + Semi-continuous mixture system of vapor phase fuel and ambient gas:

$$G_p(I) = x_F{}^p f_p(I) + \sum_{s=1}^{N} x_s{}^p \delta(I - I_s)$$

continuous phase | discrete phase

- Vapor phase transport equation,

$$\theta_p^n = \int_0^\infty I^n f_p(I) dI \qquad (n = 0, 1, 2, \cdots)$$

$$\frac{\partial}{\partial t}[\rho_f \theta_v^n] + \nabla \cdot [\rho_f \theta_v^n v] = -\nabla \cdot \int_0^\infty I^n J_I dI + S_g$$

- Assumed distribution function : Γ- func

$$f(I) = \frac{(I-\gamma)^{\alpha-1}}{\beta^\alpha \Gamma(\alpha)} \exp[-\frac{(I-\gamma)}{\beta}]$$

$$\theta = \alpha\beta + \gamma, \quad \sigma^2 = \alpha\beta^2$$

Discrete Multi-Component

- Discrete system of a liquid phase + Discrete mixture system of vapor phase fuel and ambient gas:

$$G_p(I) = \sum_{F=1}^{N_F} x_F{}^p \delta(I - I_F) + \sum_{s=1}^{N_s} x_s{}^p \delta(I - I_s)$$

discrete phase of fuel | discrete phase of air/fuel mixture

- Vapor phase transport equation,

$$\frac{\partial}{\partial t}[\rho y_i] + \nabla \cdot [\rho y_i v] = \nabla \cdot (\rho D_i \nabla y_i) + s_{g,i}$$

$$\sum \Rightarrow$$

$$\frac{\partial}{\partial t}[\rho y_F] + \nabla \cdot [\rho y_F v] = \nabla \cdot (\rho \bar{D} \nabla y_F) + S_g$$

Ra, 2009

DMC model tests

Modeled species contents*

species	MW	Mass fraction
Diesel A (US narrow-cut Diesel)		
c14h30	198	0.6253
c12h26	170	0.0559
c16h34	226	0.3025
c18h38	254	0.0163
Diesel B (Euro Diesel)		
c14h30	198	0.2376
ic8h18	114	0.0153
c10h22	142	0.0807
c12h26	170	0.1863
c16h34	226	0.1984
c18h38	254	0.2817

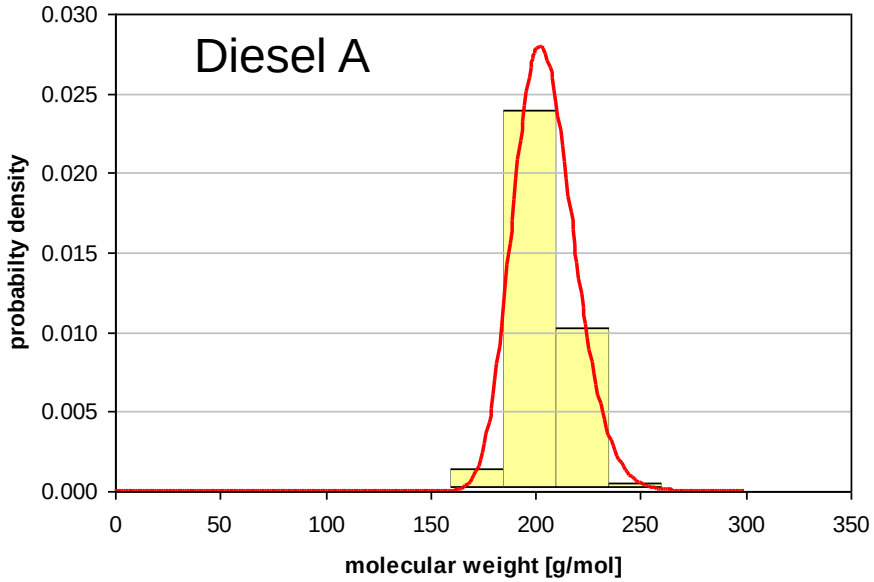

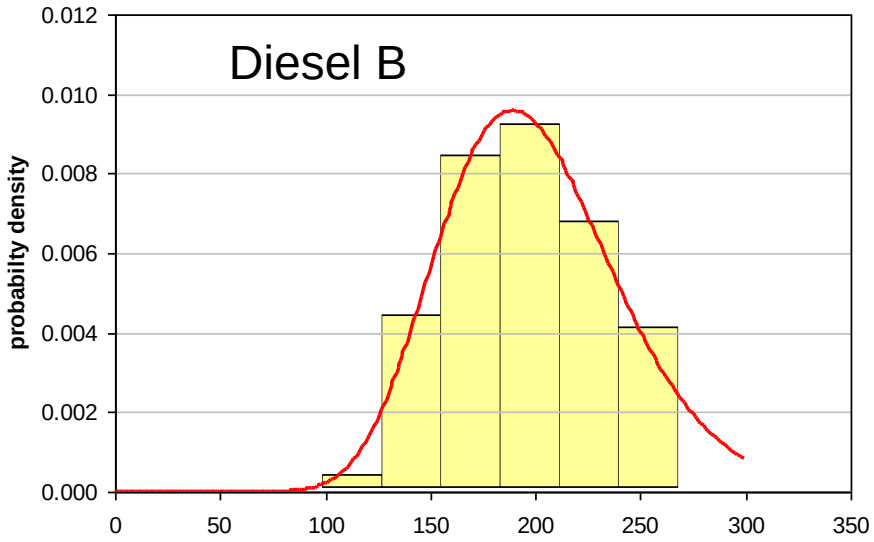

Ra, 2009

Fuel component distributions

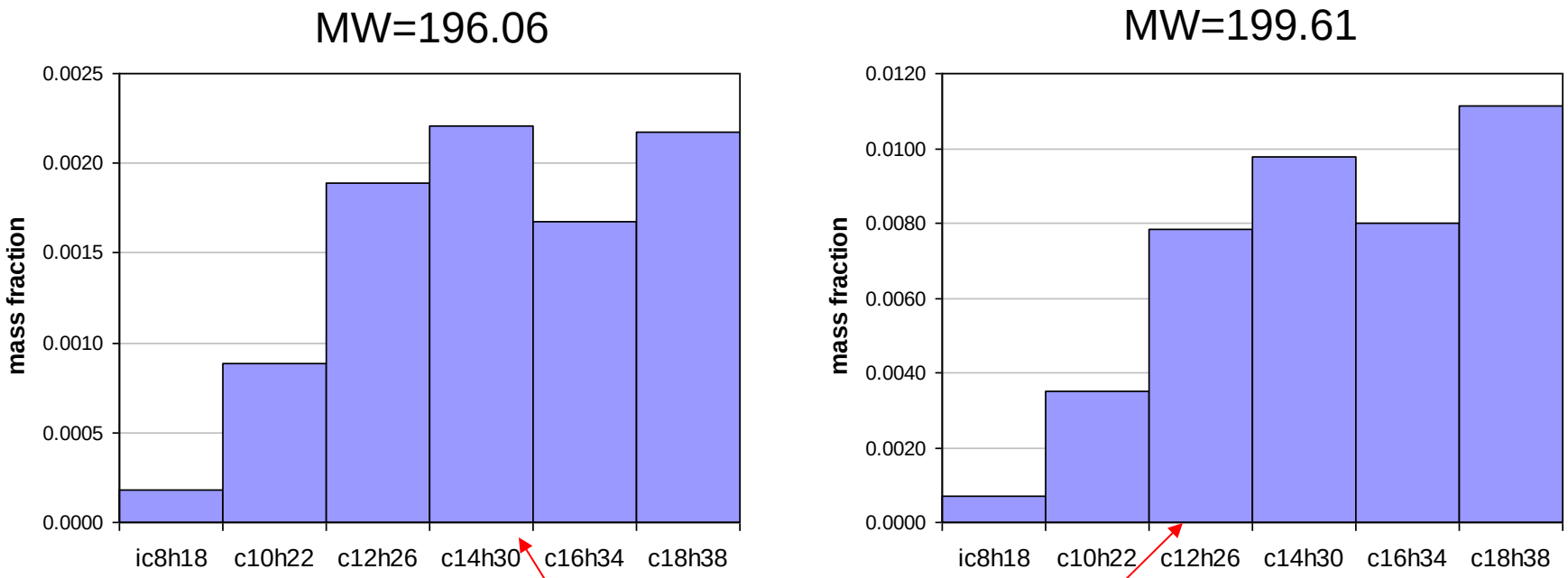

Diesel B

MW_{ini}=200

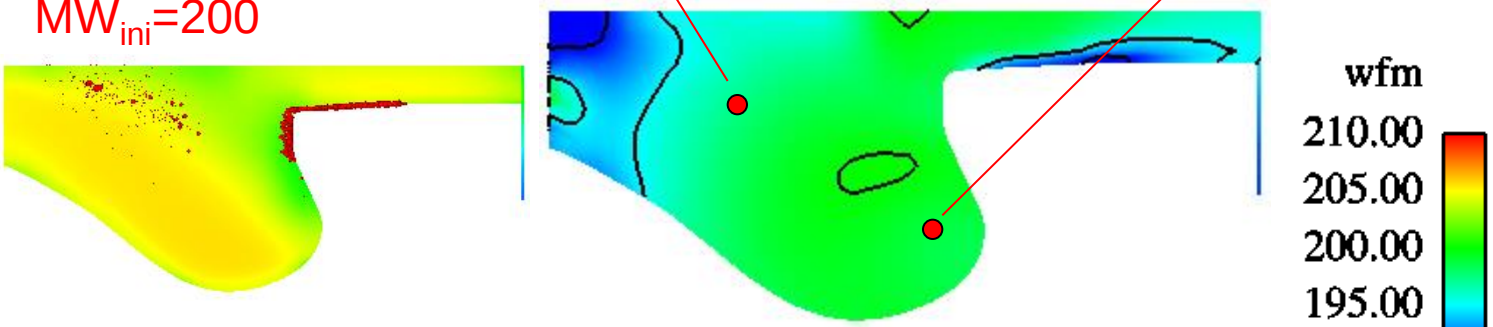

CA=-14 (~ first ignition timing)

Ra, 2009

Multi-component spray vaporization

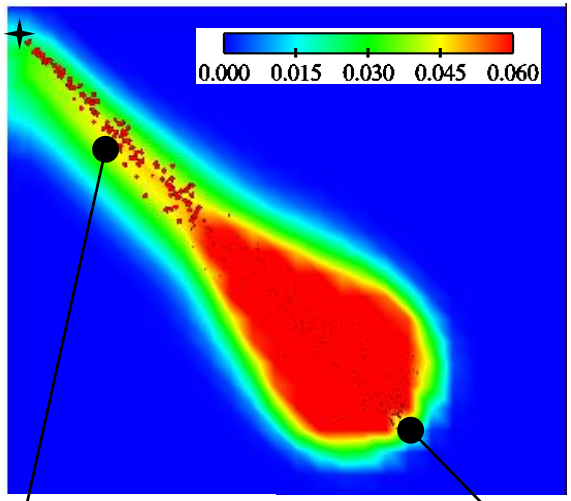

Gasoline
Do=300 μm
Vinj=100 m/s

2.0 ms after SOI

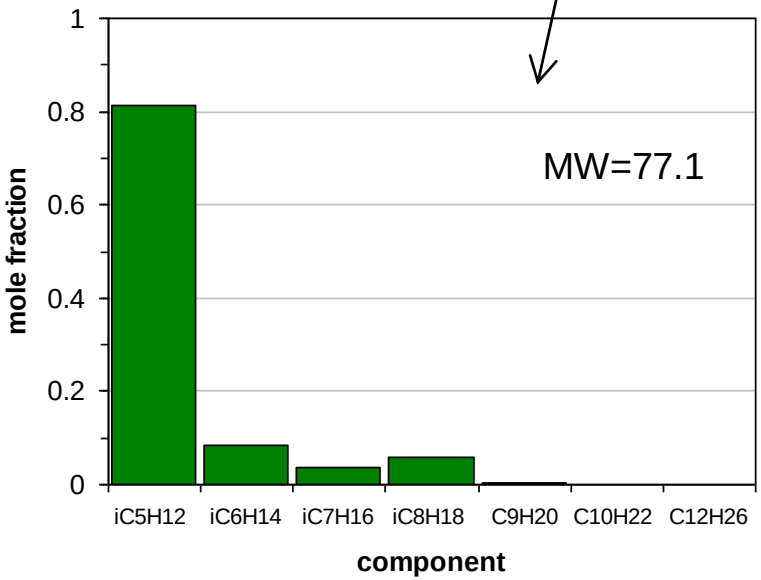

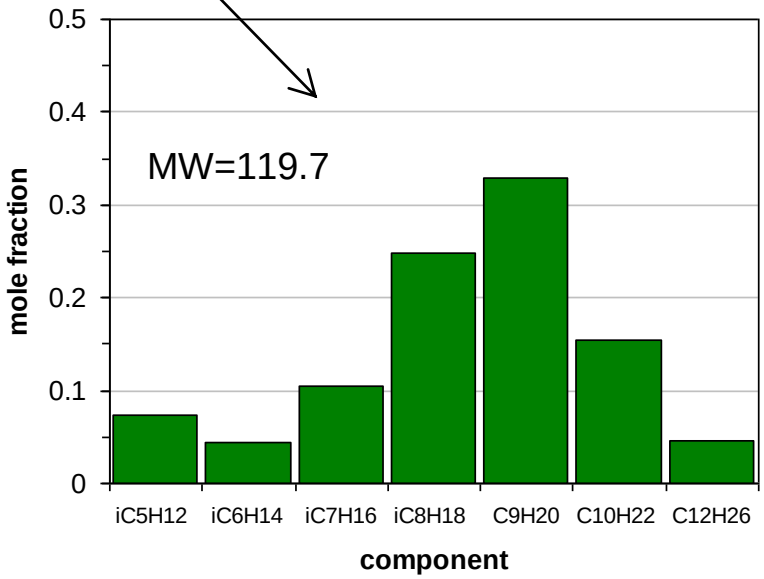

Jiao, 2011

Fredenslund, 1975

Non-ideal mixing using UNIFAC method

For mixtures composed of **polar components**, both initial and final boiling points in the distillation curve are not well predicted assuming **Ideal Mixing** (Raoult's Law) - misses the **azeotrope behavior of the mixture**.

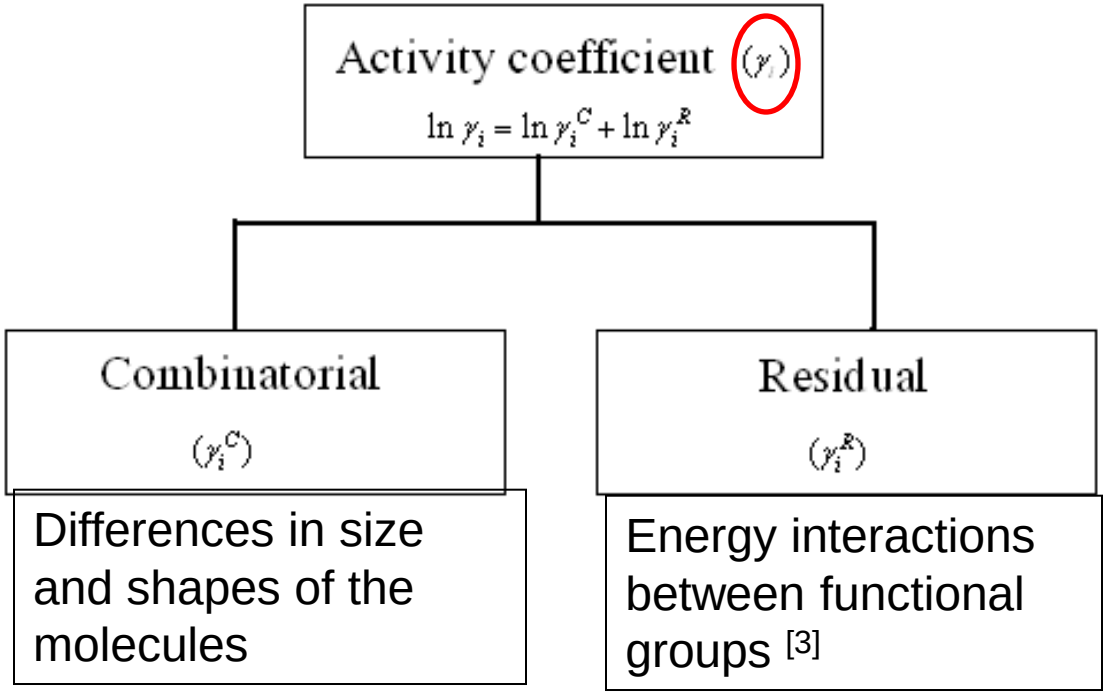

$$x_i = \frac{P_{vap,i}}{P_m}\gamma_i x_{L,i}$$

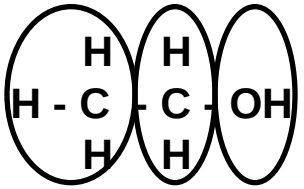

$P_{vap,i}$ Vapor pressure of pure comp. i ; P_m Total mixture pressure

$x_{L,i}$ Mole fraction of comp. i in liquid phase; x_i Mole fraction of comp. i in gas phase

Pfahl,1996
Jiao, 2011

Ethanol/gasoline surrogate mixture

Component name	Mol %			Molecular Weight [g/mol]	b.p. [^{0}C]	Functional groups in UNIFAC
Cyclo-pentane	16.8	c5h10		70.1	49	5CH2
Toluene	9.7	c7h8	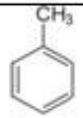	92.14	110.6	5ACH, 1ACCH3
Ethylbenzene	3.2	c8h10	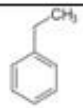	106.167	136	5ACH,1ACCH2 1CH3
meta-Xylene	4.9	c8h10	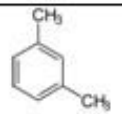	106.167	139	4ACH, 2ACCH3
n-Pentane	3.0	nc5h12		72.15	36.1	2CH3,3CH2
n-Heptane	3.6	nC7h16		100.21	98.42	2CH3,5CH2
Isopentane	7.8	ic5h12		72.15	27.7	3CH3,1CH2 1CH
isoheptane	7.7	ic7h16		100.20	90.0	3CH3,3CH2, 1CH
iso-octane	2.5	ic8h18	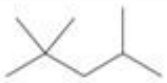	114.23	99.3	5CH3,1CH2, 1CH,1C

Jiao, 2011

Drop evaporation simulation

- Droplet lifetime

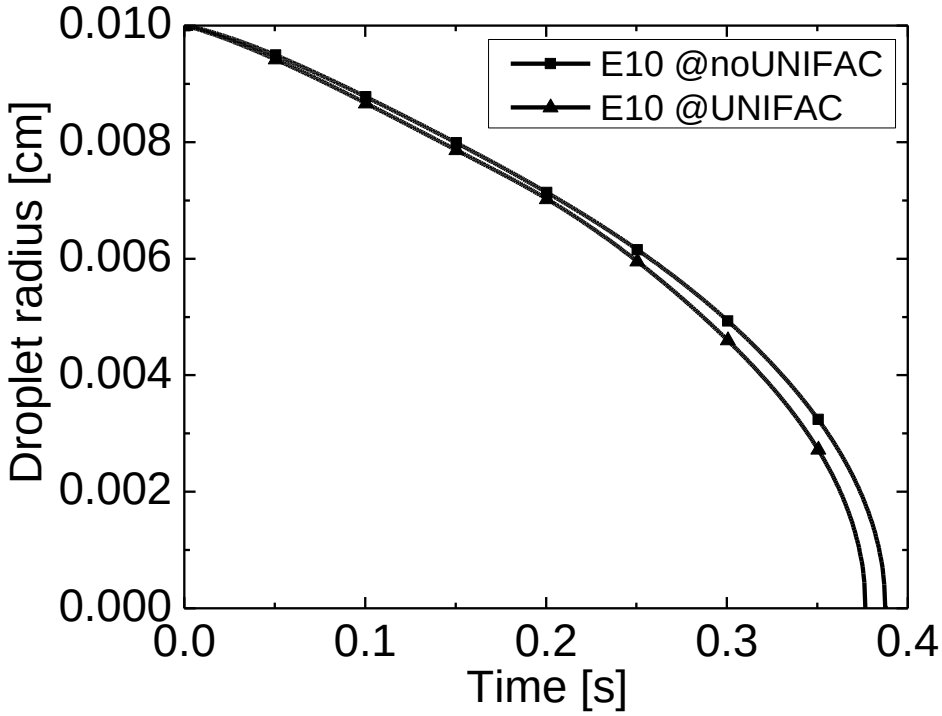

- Temp. vs. mole fraction

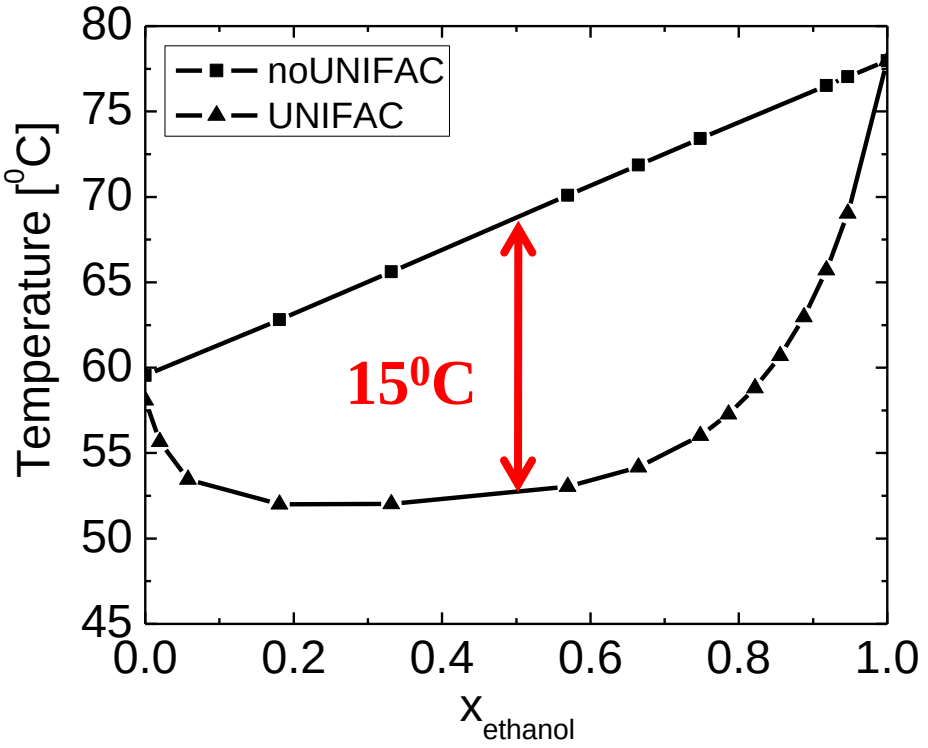

Jiao, 2011

Andersen, 2010

Distillation curve

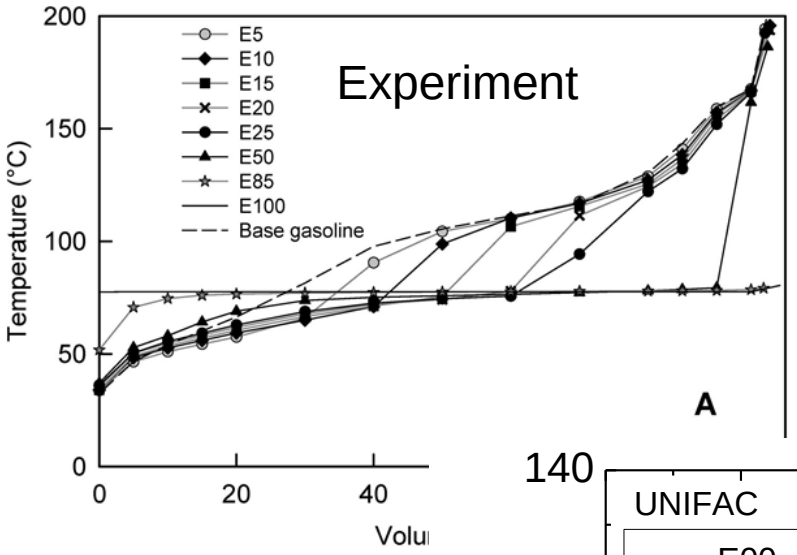

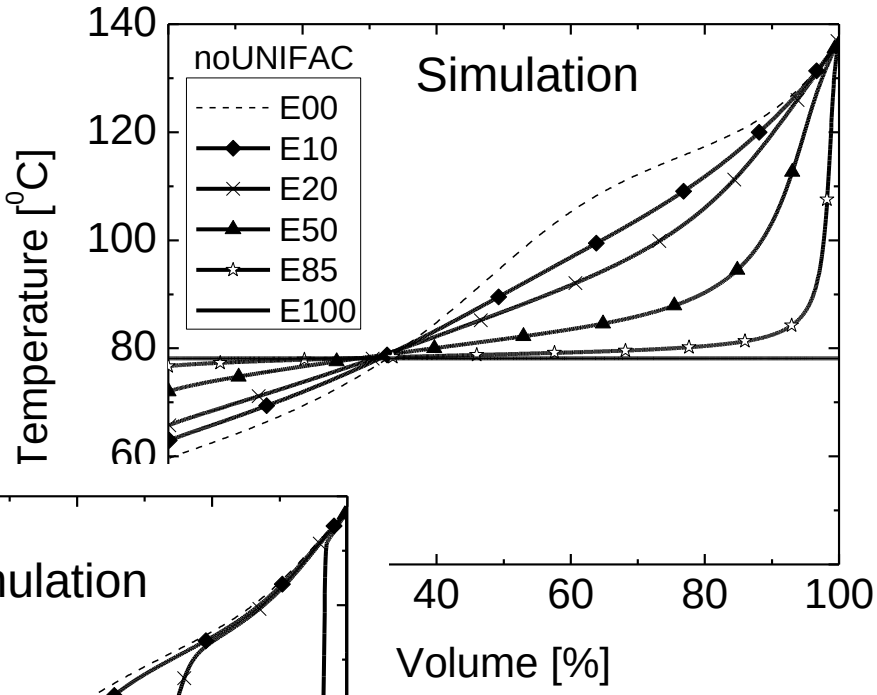

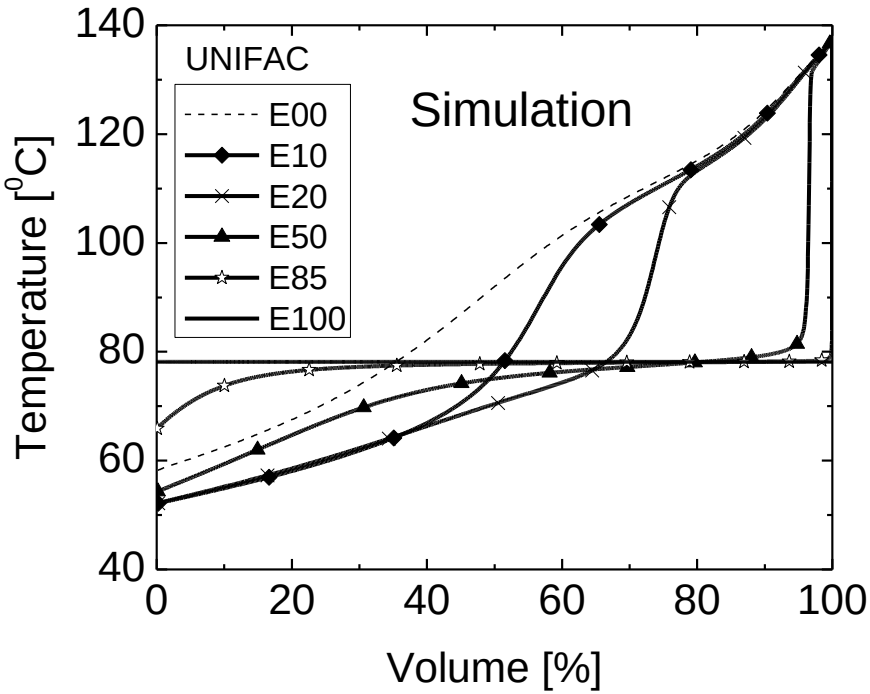

E20 has the lowest initial boiling temperature

Anand, 2011

Surrogate fuels - 18 component model

	diesel	Jet-A	JP-8
cyC6	0.010000	0.022529	0.012529
c7h8	0.037698	0.035873	0.025873
c10h8	0.020000	0.009607	0.0
c10h18	0.0	0.0	0.030000
c10h22	0.113977	0.253797	0.721022
c12h26	0.124544	0.298704	0.118311
c14h10	0.0	0.0	0.0
c14h30	0.210805	0.202265	0.022265
c16h34	0.172593	0.060627	0.0
c18h38	0.085615	0.0	0.0
c20h42	0.084268	0.0	0.0
mxylene	0.010000	0.079442	0.0
mcymene	0.050355	0.0	0.0
c11h16	0.0	0.019881	0.0
tetralin	0.017362	0.017275	0.0
c12h18	0.017362	0.0	0.0
c13h20	0.045421	0.0	0.0
nc7h16	0.0	0.0	0.070000

alkanes

aromatics

cycloalkanes

PAH

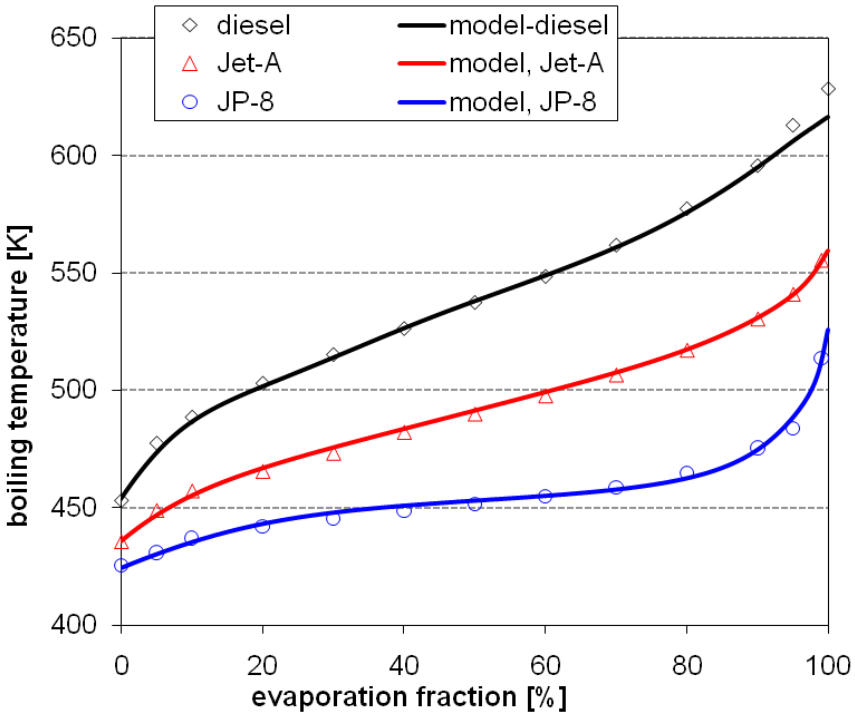

	Diesel	Model-Di	Jet-A	Model-JetA	JP-8	Model-JP8
Density [g/cm^3]	0.8478	0.7800	0.8101	0.7638	0.7547	0.7333
Viscosity [cSt]	2.71	2.05	1.55	1.36	1.15	1.01
Surface tension [dynes/cm]	30	26.91	29.1	25.53	25.2	23.64
LHV [kJ/kg]	42526	42527.7	43305	43306.6	44185	44199.4
Saturates [%]		81.4	84.4	83.7	94.7	94.1
Aromatics [%]		17.6	14.0	14.1	1.2	2.2
Olefins [%]			1.6		4.1	
Naphthenes [%]		1.0		2.2		3.7
C/H ratio	6.852	6.102	6.534	5.997	5.95	5.565
Molecular weight [g/mol]	190	177	160	152	150	139

← corrected

Anand, 2011

Diesel hydrocarbon class distributions and surrogates

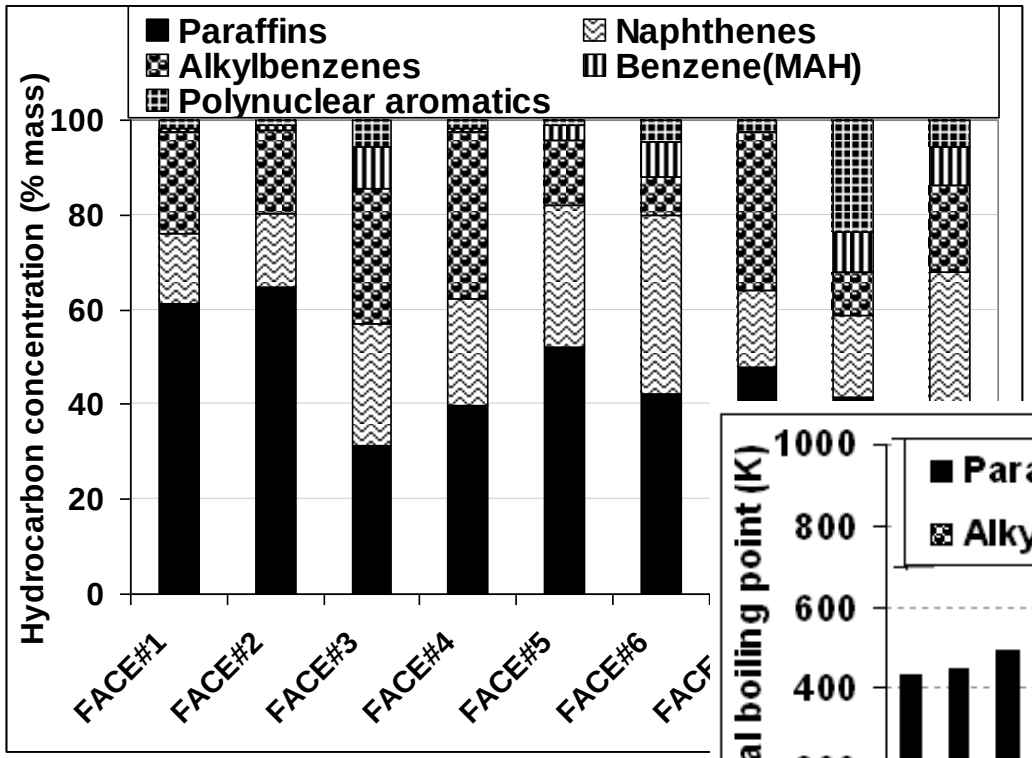

FUELS for Advanced Combustion Engines (FACE)

Measured hydrocarbon class distributions

20 species physical property surrogate database

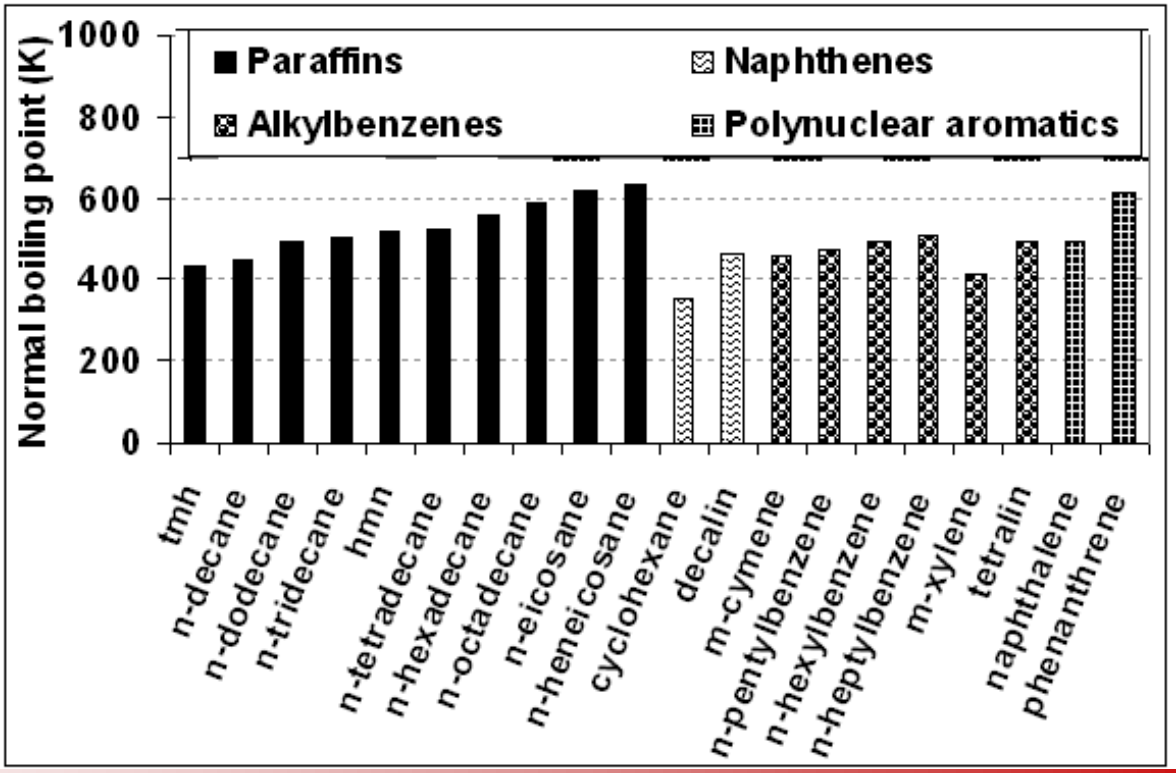

* Anand, 2011

Chemical structure and activity coefficients of Face #9 surrogates

component	chemical structure	activity coefficient γ at 373 K
n-Tetradecane ($C_{14}H_{30}$)		1.01
Cyclohexane (C_6H_{12})		0.88
Decalin ($C_{10}H_{18}$)	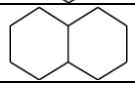	1.03
n-Decane ($C_{10}H_{22}$)		1.06
n-Hexadecane ($C_{16}H_{34}$)	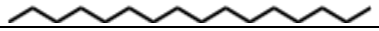	0.95
n-Eicosane ($C_{20}H_{42}$)		0.81
Phenanthrene ($C_{14}H_{10}$)	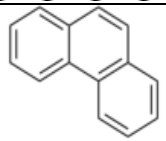	2.22
m-Xylene (C_8H_{10})	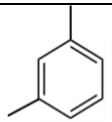	1.06
m-Cymene ($C_{10}H_{14}$)	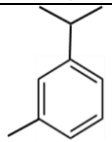	1.07
Pentylbenzene ($C_{11}H_{16}$)	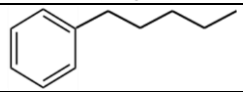	1.08
Tetralin ($C_{10}H_{12}$)	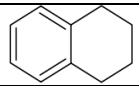	1.17
Heptylbenzene ($C_{13}H_{20}$)	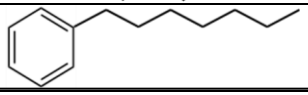	1.10

Departure from Raoult's law - Non-ideal vaporization influences heavy-end of distillation curve *

$$p_{i,v} = x_{i,v}P$$
$$= x_{i,l}\gamma_i P_{sat,i}$$

Anand, 2011

Example - face fuel #1 surrogate composition

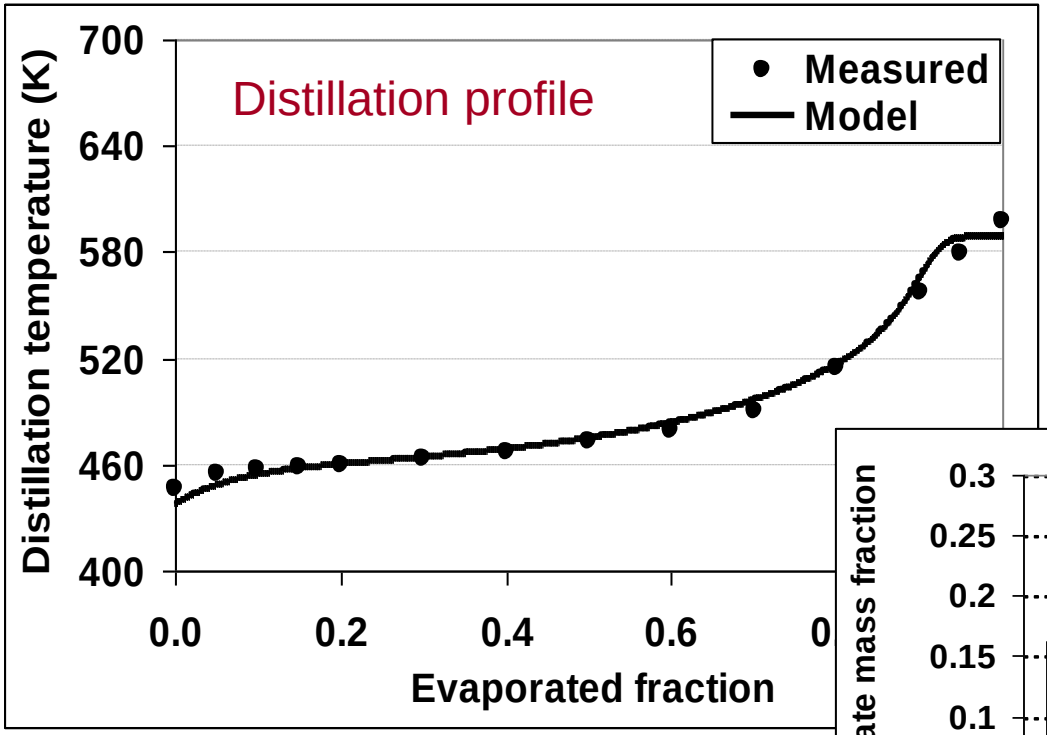

Batch distillation modeled as flash boiling droplet

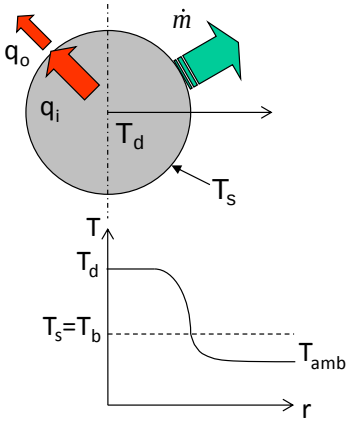

Physical property surrogates

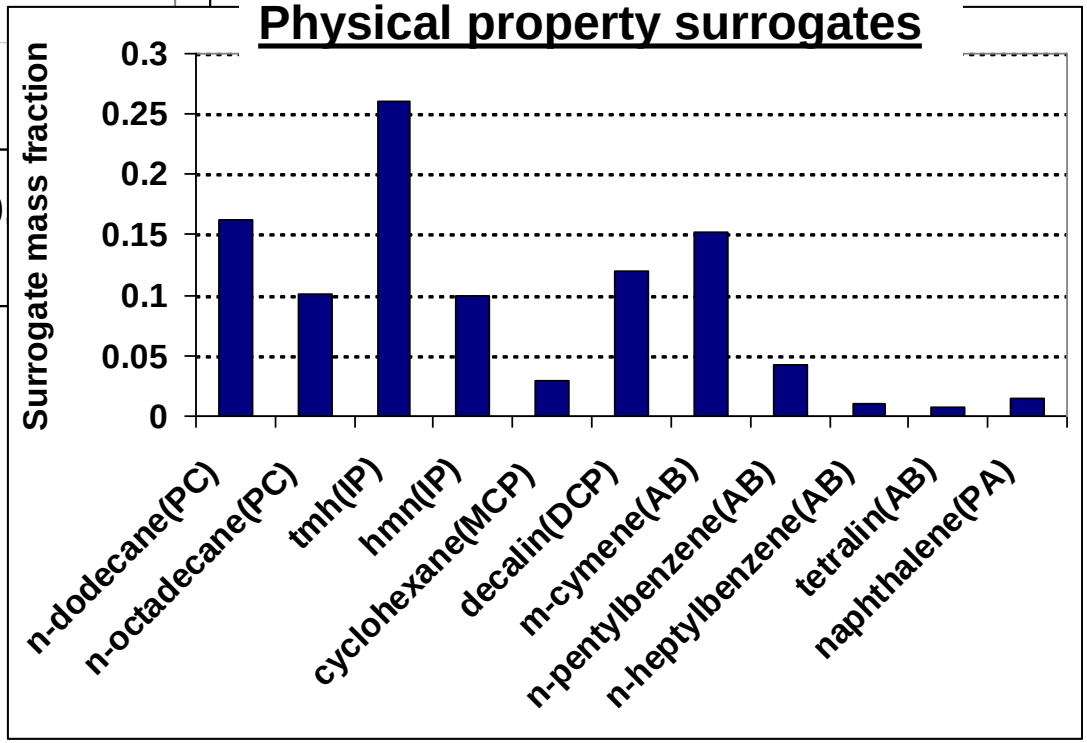

Chemical classes

PC – normal paraffins
IP – iso-paraffins
MCP – mono cyclo paraffins
DCP – di-cycloparaffins
AB – Alkyl benzenes
PA – poly aromatics

Abani, 2008

Putting them all together - Grid independent spray models

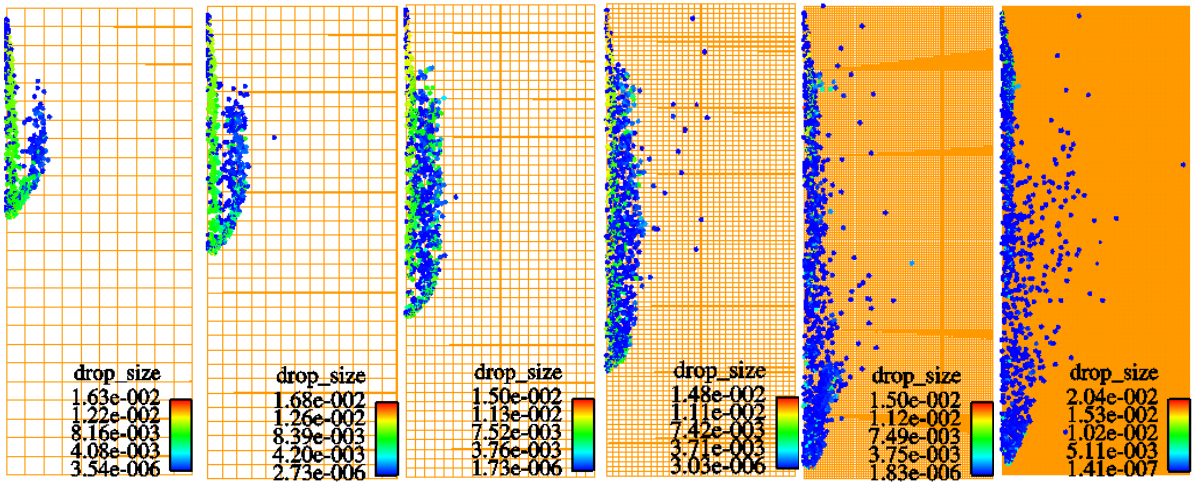

4 mm 3mm 2 mm 1 mm 0.5 mm 0.25m

Gas-jet sub-grid momentum exchange near nozzle

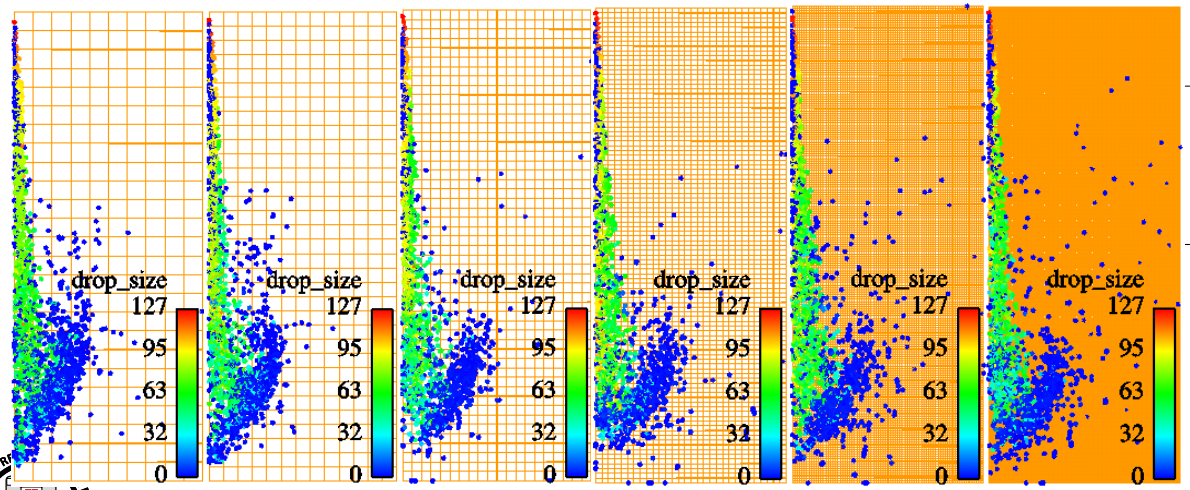

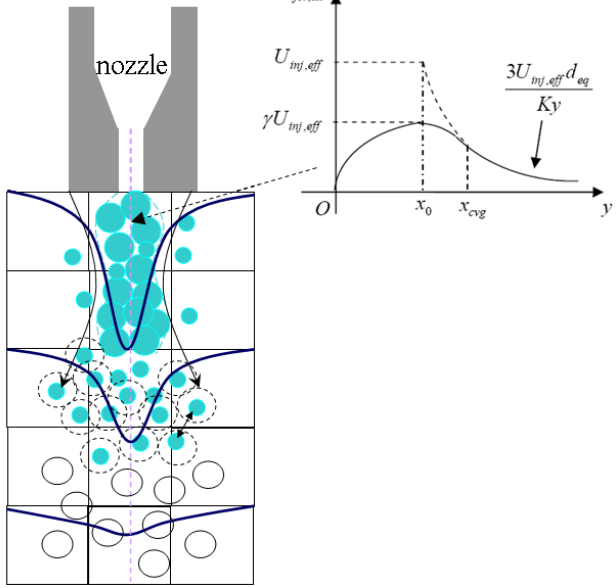

Coarse mesh:
Drop drag over-predicted

Fine mesh:
Drop coalescence under-predicted

Wang, 2010

Spray model validation

6-hole injector; Iso-octane; constant volume chamber, cold ambient; Injection pressure: 120, 200bar; chamber pressure: 12bar;

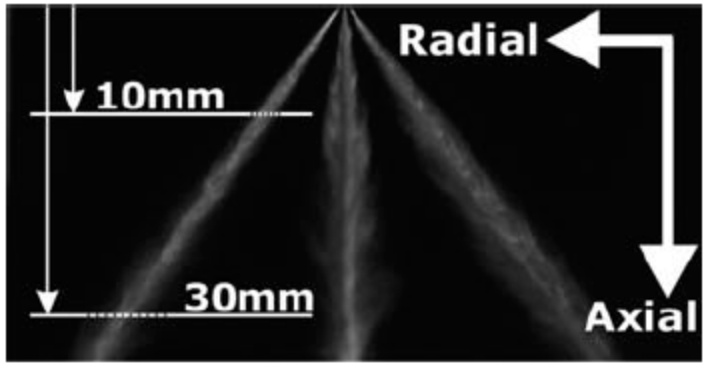

Expts: Mitroglou, 2006

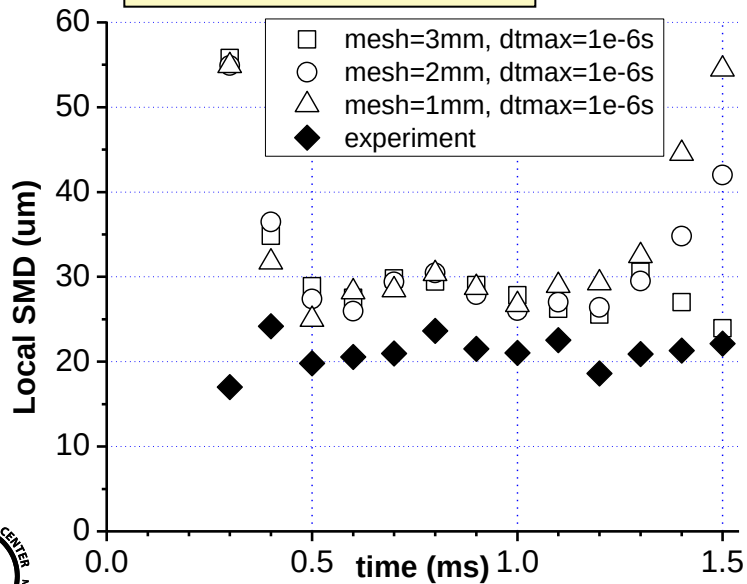

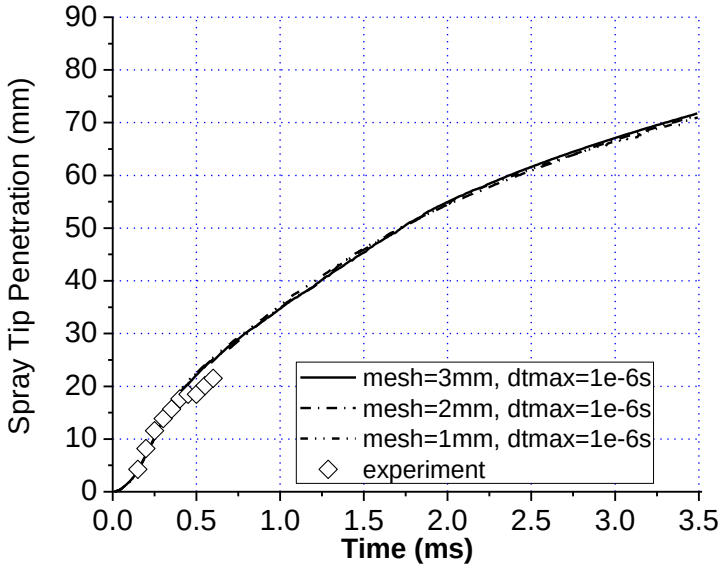

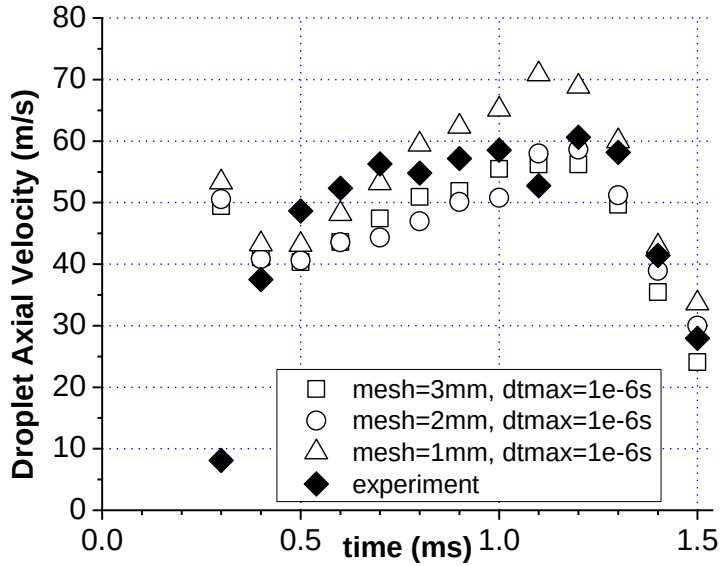

Naber, 1996

Siebers, 1998

Validation – evaporating sprays

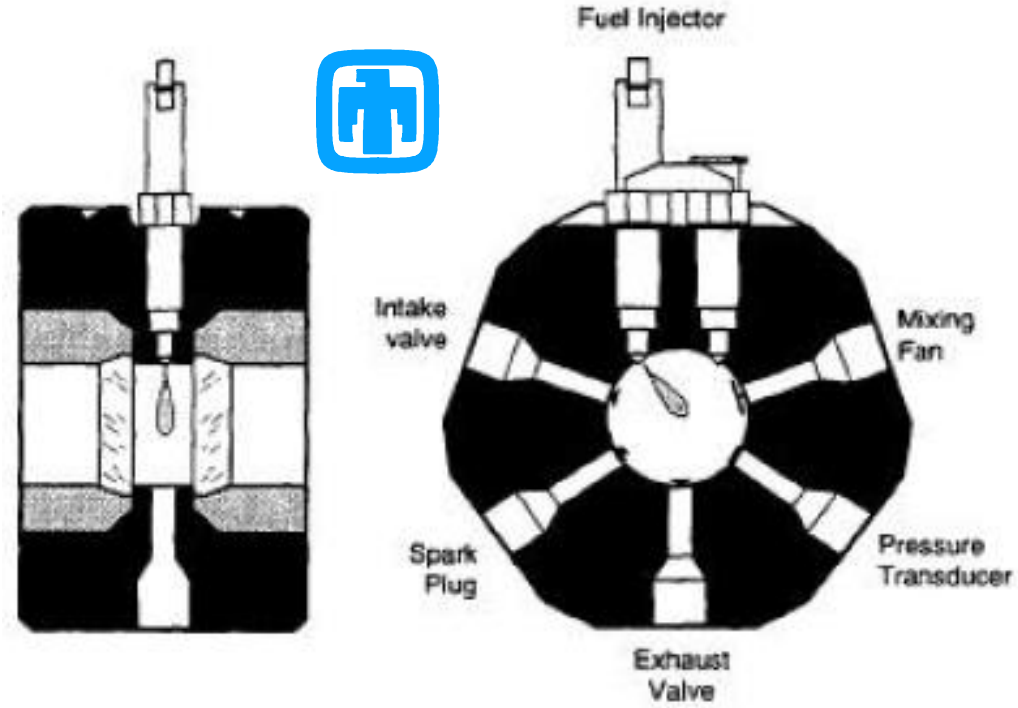

Diesel and other fuels;

Constant volume chamber; various temperatures;

Varying chamber densities: 13.9, 28.6, 58.6kg/m^3.

Schlieren imaging

Pickett, Sandia National Laboratory, "Engine Combustion Network", https://share.sandia.gov/ecn/

Wang, 2010

Evaporating diesel spray – grid size and time step independency

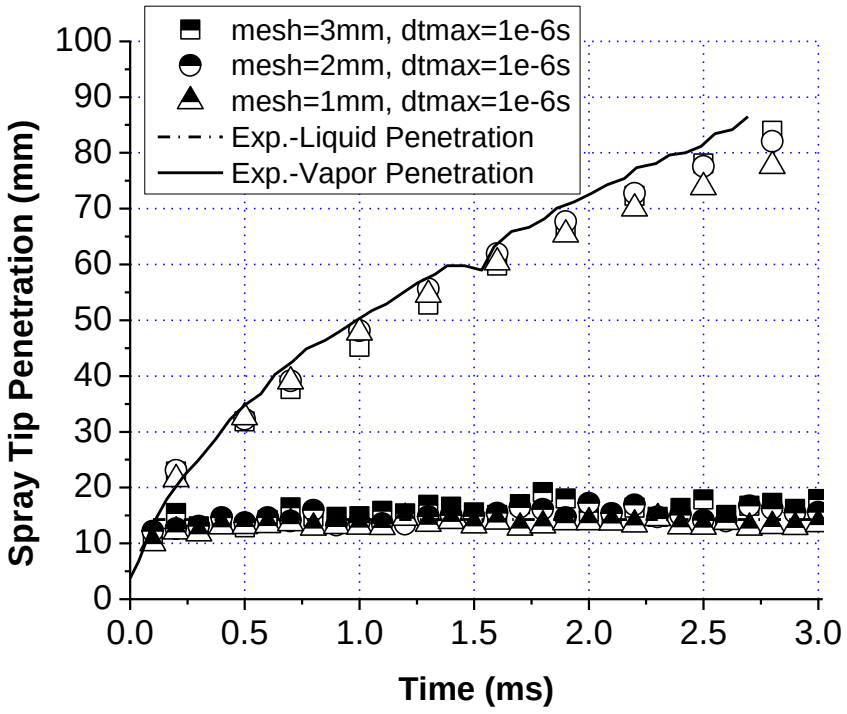

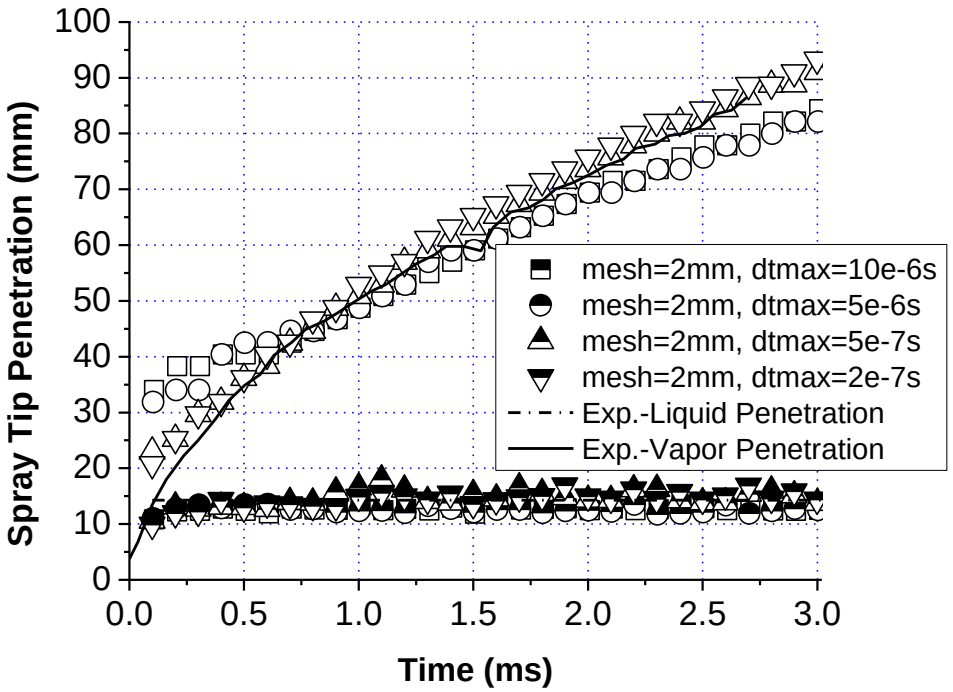

Predicted vapor and liquid penetrations.
Experimental data of Naber and Siebers (1996) and Pickett (2007).
Diesel fuel injection, nozzle diameter 257 mm, injection pressure 1370bar, gas temperature 1,000K, gas density 58.6 kg/m^3 .

Juneja, 2004

Evaporating diesel spray - liquid length

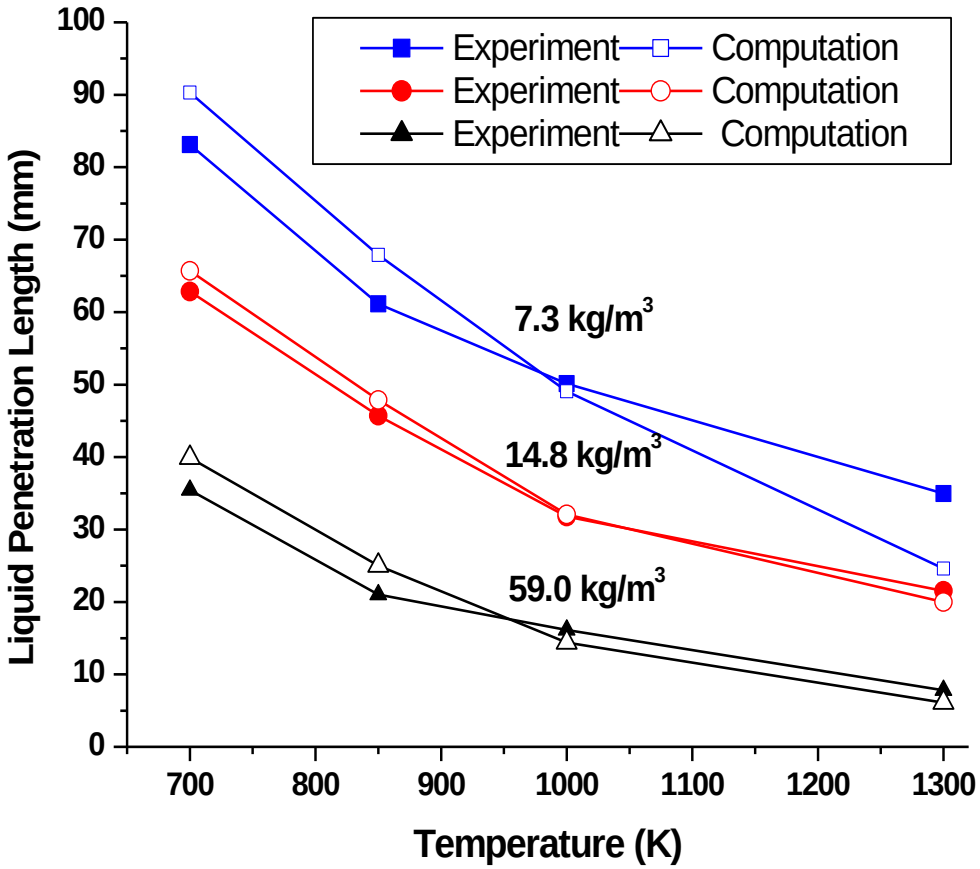

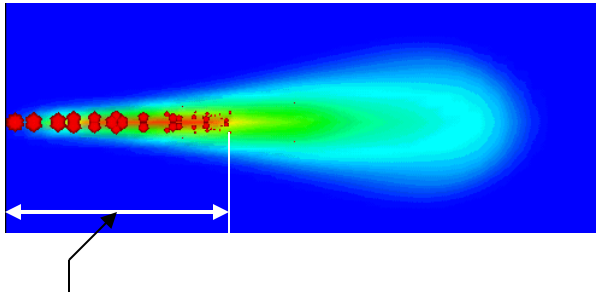

Siebers, 1998

Injection Pressure : 135 MPa

Fuel : DF2

Orifice Diameter : 246 μm

Comparison of model results with experimental liquid penetration length data

Wang, 2014

ECN Spray A modeling

Temp [K]	800	850	900	1000	1100	1200
O_2 [vol%]	15	13/15/17/21	13/**15**/17/21	13/15/17/21	13/15/17/21	13/15/17/21
Density [kg/m^3]	22.8	7.6/15.2/ 22.8/30.4	7.6/15.2/ **22.8**/30.4	7.6/15.2/ 22.8/30.4	7.6/15.2/ 22.8/30.4	7.6/15.2/ 22.8/30.4
P_{inj} [MPa]	150	50/100/150	50/100/**150**	50/100/150	50/100/150	50/100/150

Computational grid

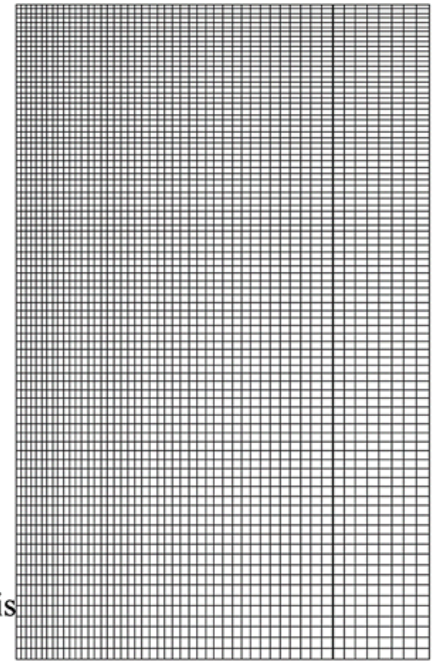

Related sub-models

Phenomenon	Model
Spray breakup	KH-RT instability
Evaporation	Discrete multicomponent (DMC)
Turbulence	Generalized RNG k−ε model
Combustion	SpeedChem
Droplet collision	ROI model
Near nozzle flow	Gas-jet model
Soot formation	Multi-step phenomenological

Lift-off length

Onset of the averaged OH concentration

Ignition delay

Maxmium d*T*/d*t*
Maxmium d*OH*/d*t*

Wang, 2014

ECN Spray A modeling

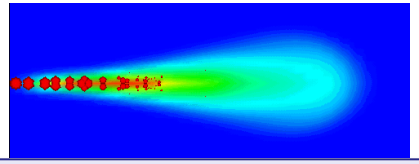

Non-reacting mixing process

Ambient conditions	
O2	0.0
N2	0.8971
CO2	0.0652
H2O	0.0377
Pressure	60.45 bar
Temperature	900 K
Density	22.8 kg/m^3
Injector specifications	
Type	Common-rail
Nozzle	Single-hole, 0.89
Nozzle diameter	0.084 mm (0.090mm)
Injection pressure	150 MPa
Injection duration	6.0 ms
Injection fuel mass	13.77 mg

Liquid and vapor penetrations[1]

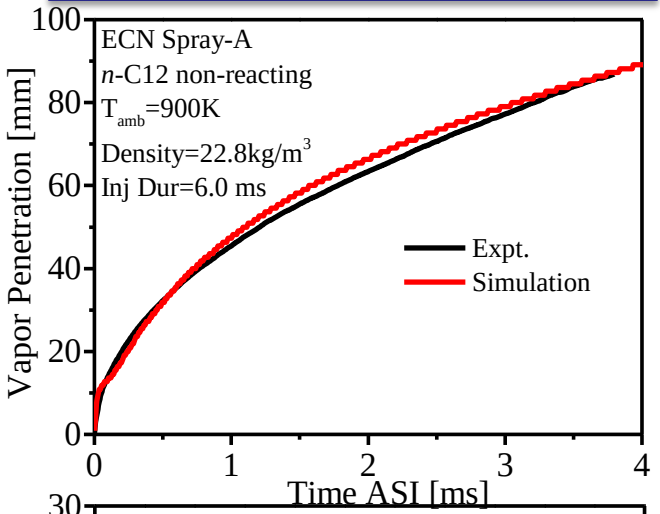

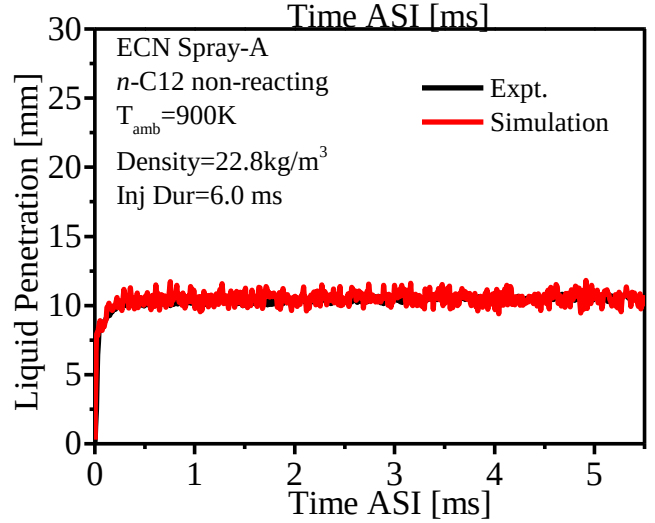

1. Engine Combustion Network, http://www.sandia.gov/ecn/

Wang, 2014

Vishwanathan, 2010

ECN Spray A modeling

Physical process	Expression
Inception:A_4→soot	$C_{16}H_{10}(A_4) \xrightarrow{\dot{\omega}_1} 16C(s) + 5H_2$
C_2H_2 surface growth	$C(s) + C_2H_2 \xrightarrow{\dot{\omega}_2} 3C(s) + H_2$
Coagulation	$nC(s) \xrightarrow{\dot{\omega}_3} C(s)_n$
O_2 oxidation	$C(s) + \frac{1}{2}O_2 \xrightarrow{\dot{\omega}_4} CO$
OH oxidation	$C(s) + OH \xrightarrow{\dot{\omega}_5} CO + \frac{1}{2}H_2$
PAH condensation	$C(s) + PAH_{i,j} \xrightarrow{\dot{\omega}_6} C(s+k) + \frac{j}{2}H_2$
Transport equations	$\frac{\partial M}{\partial t} = -\nabla \cdot (M \cdot v) + \nabla \cdot \left(\frac{\mu}{SC} \nabla \left(\frac{M}{\rho} \right) + \xi \cdot M \cdot \frac{\mu}{\rho} \frac{\nabla T}{T} \right) + \dot{S_M}$

Source term:

Mass: $\dot{S_M} = (16\dot{\omega}_1 + 2\dot{\omega}_2 + 6\dot{\omega}_6 - \dot{\omega}_4 - \dot{\omega}_5) \quad [g\ cm^3 s^{-1}]$

Number density: $\dot{S_M} = \left(16\dot{\omega}_1 \cdot \frac{M_{C(s)}}{M_{unci}} - \dot{\omega}_3\right) \quad [particles\ cm^3 s^{-1}]$

Wang, 2013

Reaction mechanism -formulation

n-$C_{12}H_{26}$-PAH mechanism

104 species and 444 reactions
- Reduced *n*-dodecane mechanism

80 species and 299 reactions
- Reduced PAH mechanism

42 species and 228 reactions[1]

PAH mechanism

- **A1 formation**

$C_3H_3+C_3H_3=C_6H_6$

$C_3H_3+C_3H_3=C_6H_5+H$

$C_4H_5+C_2H_2=C_6H_6+H$

$C_4H_3+C_2H_2=C_6H_5$

- **Larger PAH formation**

1. HACA sequence
2. Small radical and molecule
3. Addition reactions between aromatic radicals and molecules

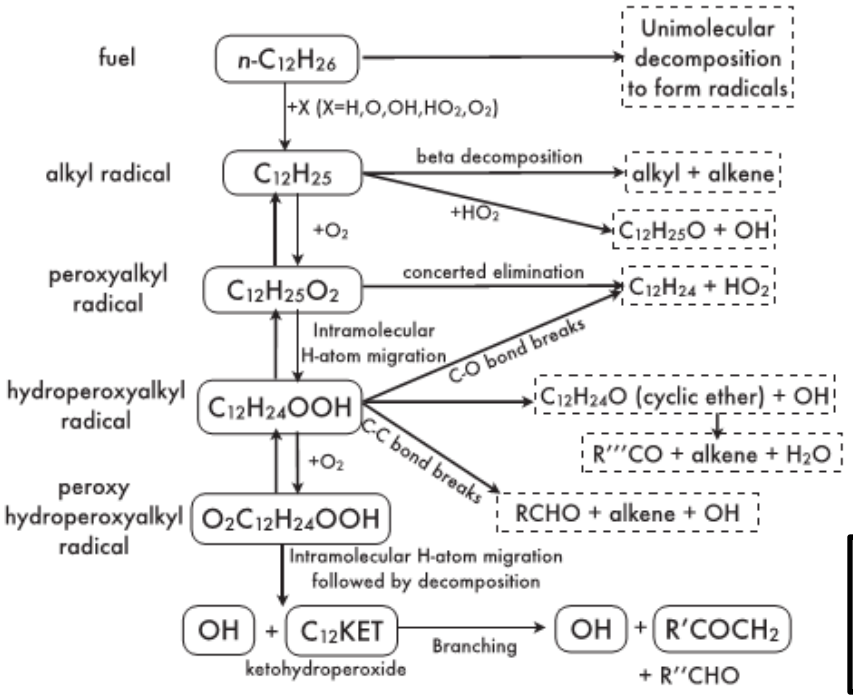

n-C12 reaction pathway

PAH mechanism validation

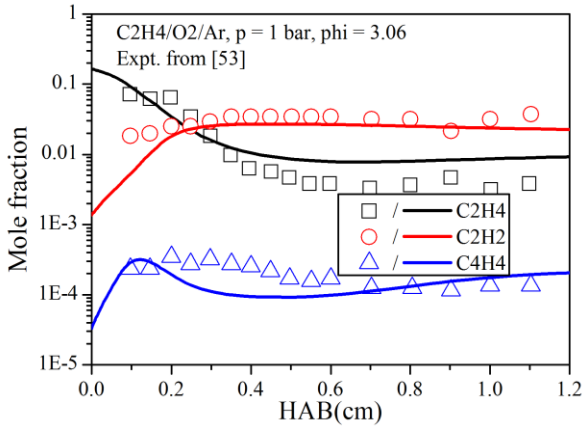

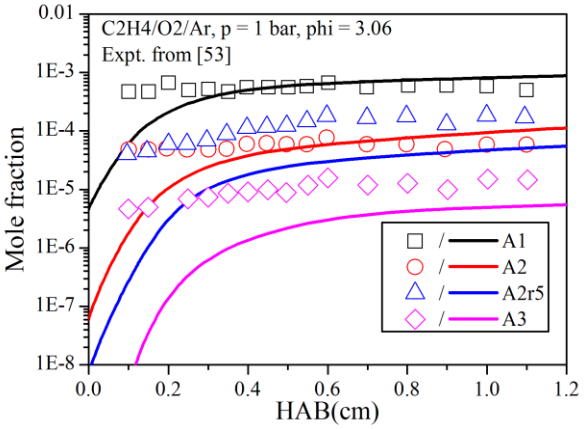

Wang, 2013

Reaction mechanism -validation

Ignition delay[1]

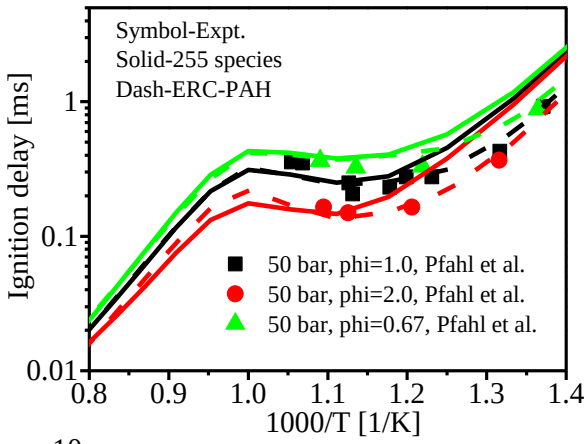

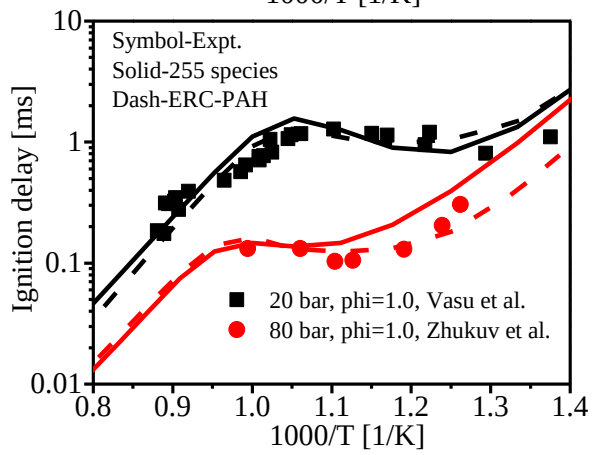

Shock Tube[2]

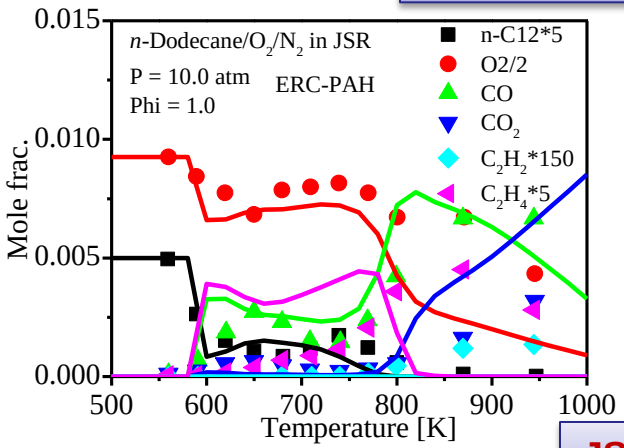

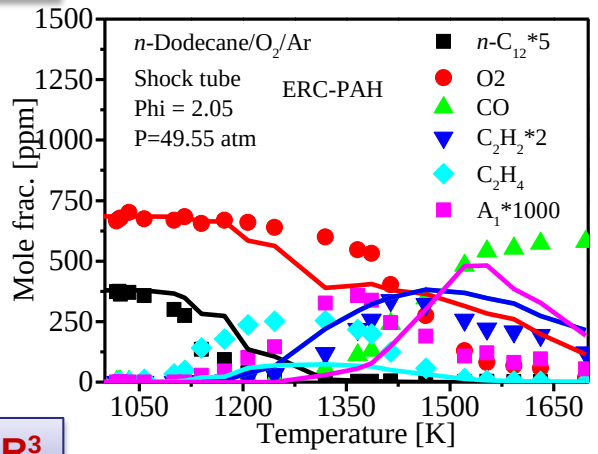

JSR[3]

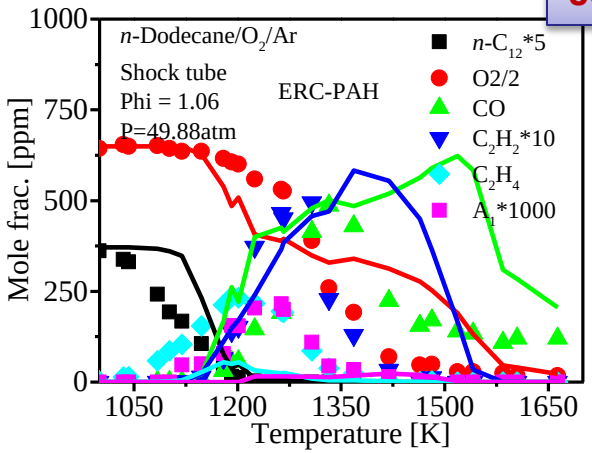

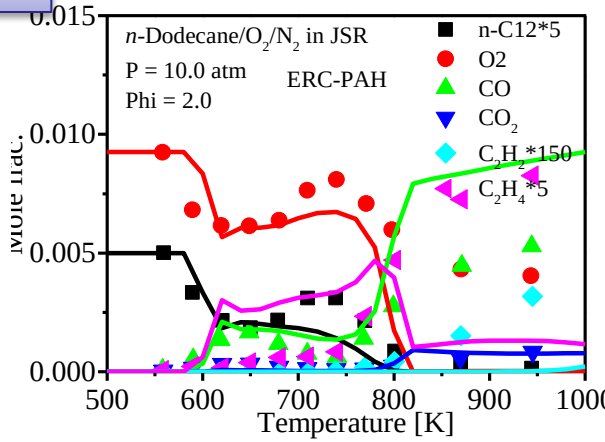

1. Narayanaswamy, 2014
2. Mzé-Ahmed, 2012
3. Malewicki, 2013

Wang, 2014

ECN Spray A modeling

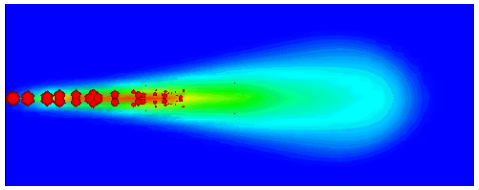

Non-reacting mixing process - Fuel mixture fraction

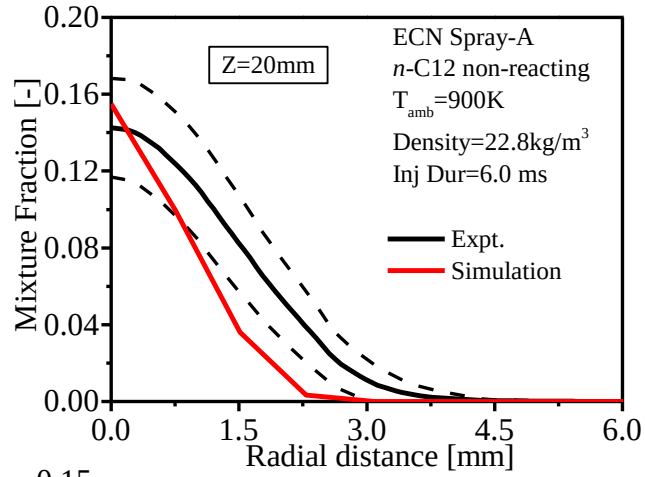

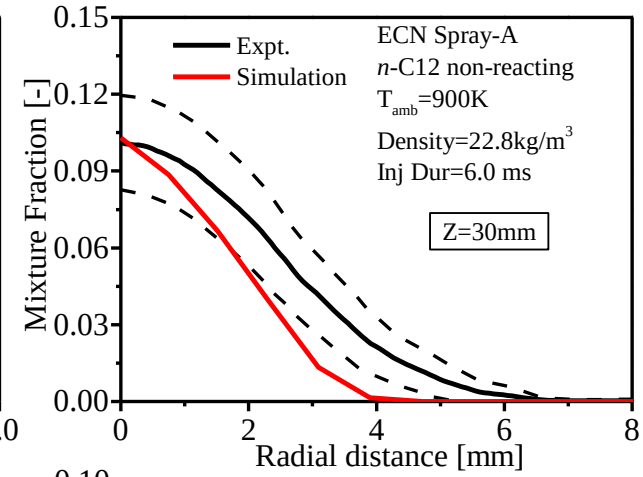

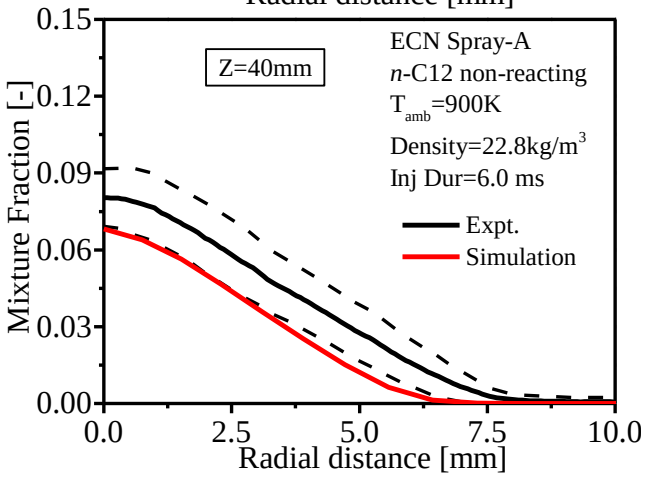

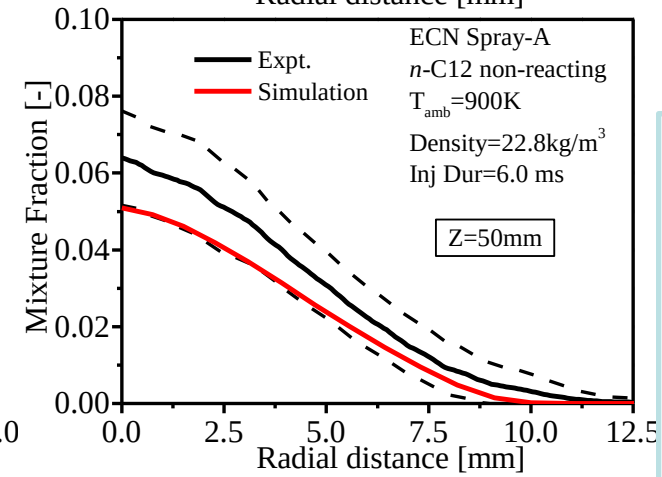

Axial

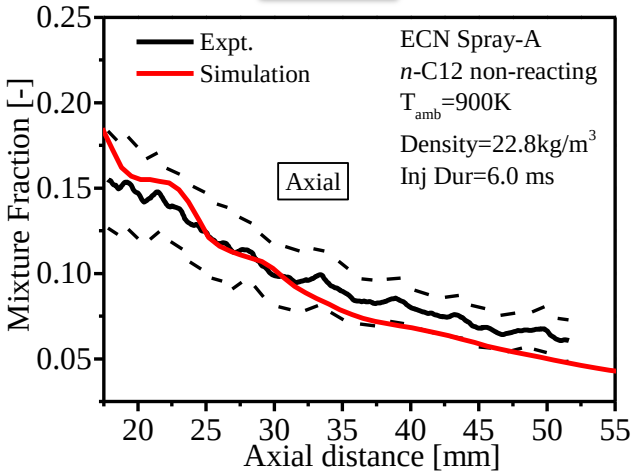

- ✓ Predicted mixture fraction distributions agree reasonable well with experimental data in both radial and axial directions by calibrating the spray model constants

1. Engine Combustion Network, http://www.sandia.gov/ecn/

Wang, 2014

Skeen, 2013

Reacting conditions - Soot formation vs. Ambient temperature

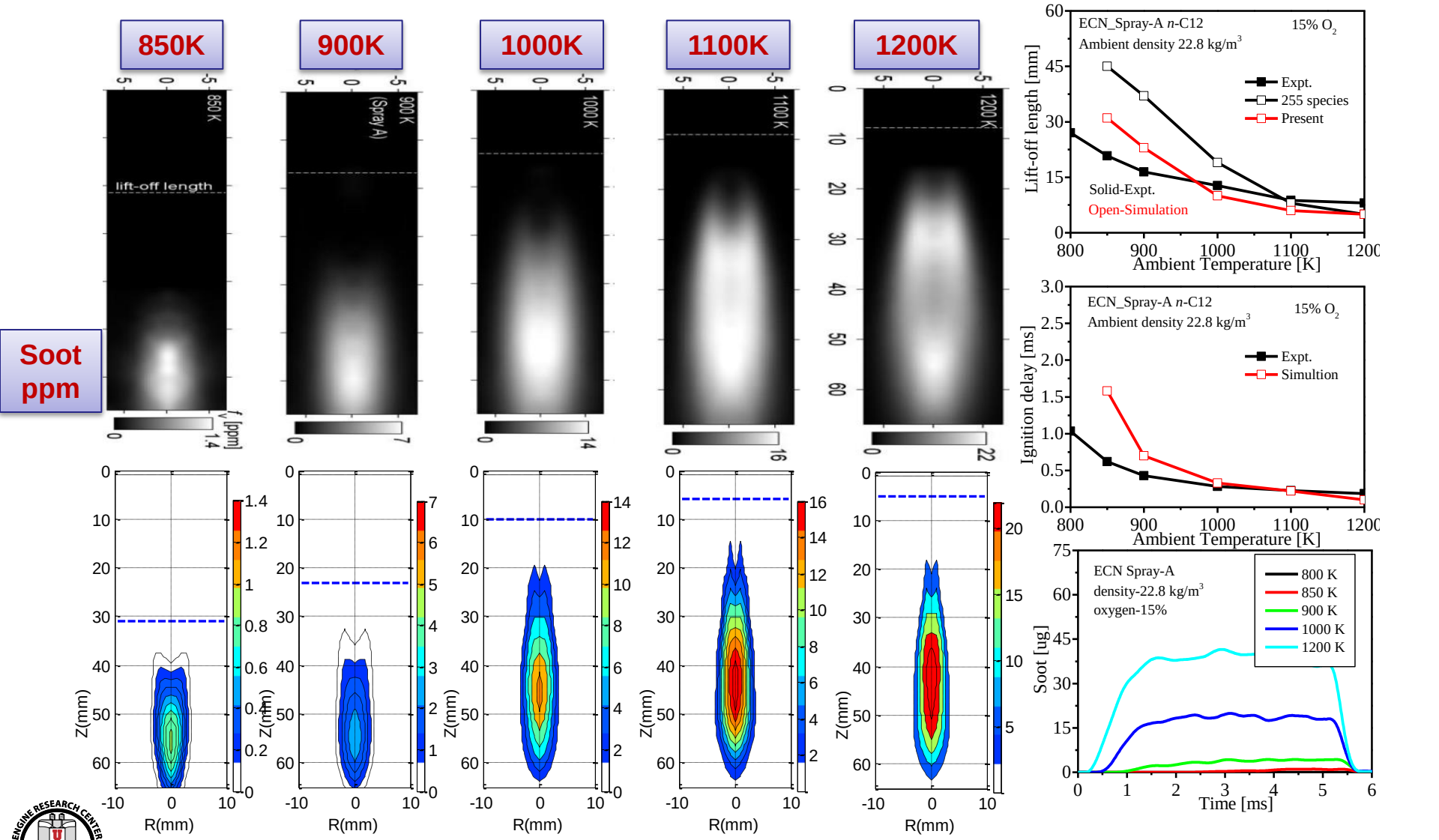

Wang, 2014

ECN Spray A modeling

Soot ppm

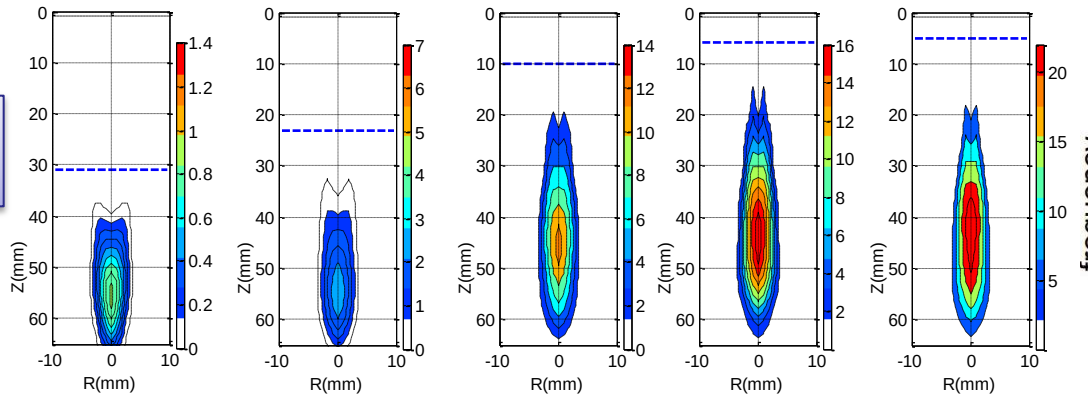

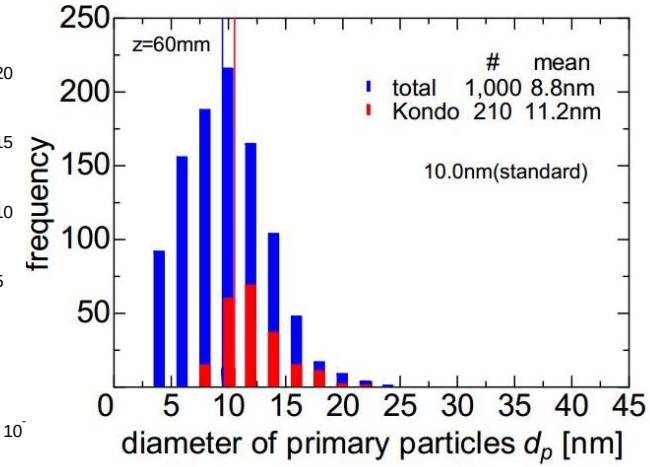

A_4

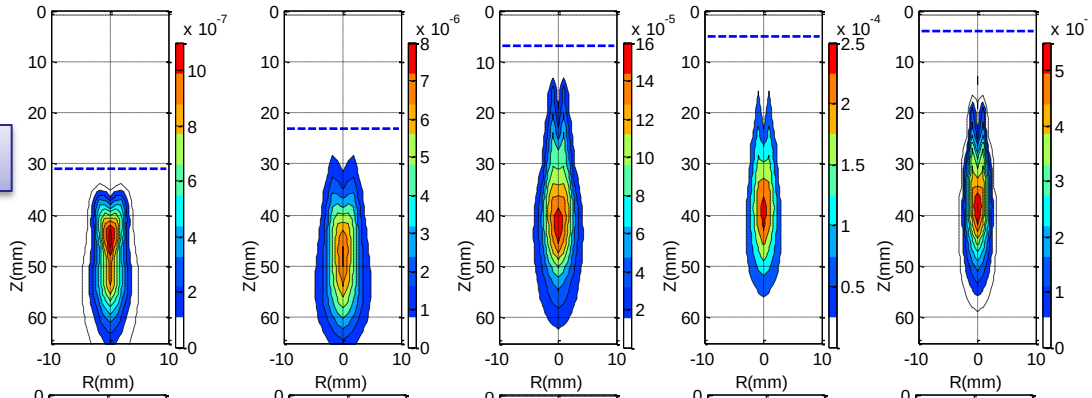

D_{soot}

Peak 16 nm

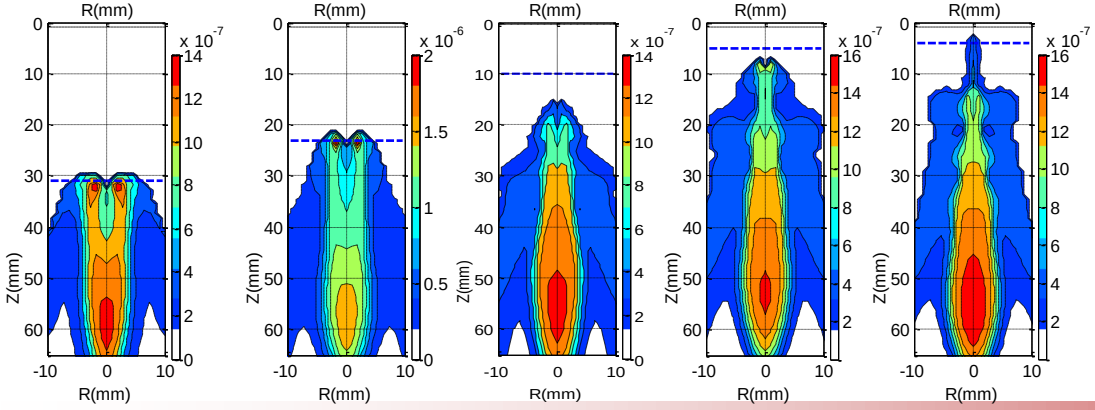

- The soot formation regions agree with the high A_4 concentration regions;
- Predicted soot particle size is in the reasonable range compared to experimental data;

Wang, 2014

Reacting conditions - Soot formation Overview

Total soot mass @4.5ms

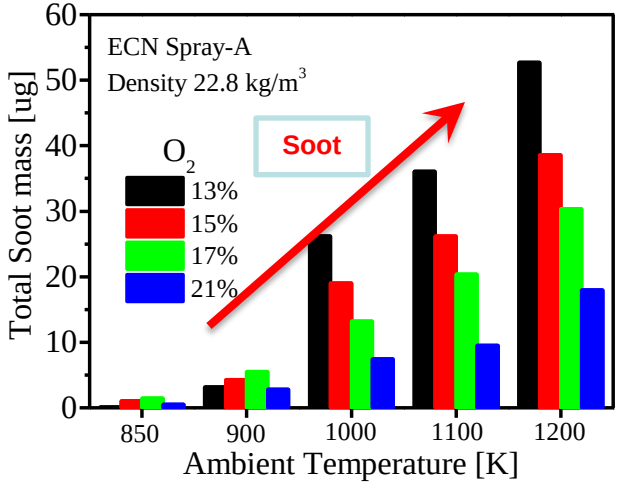

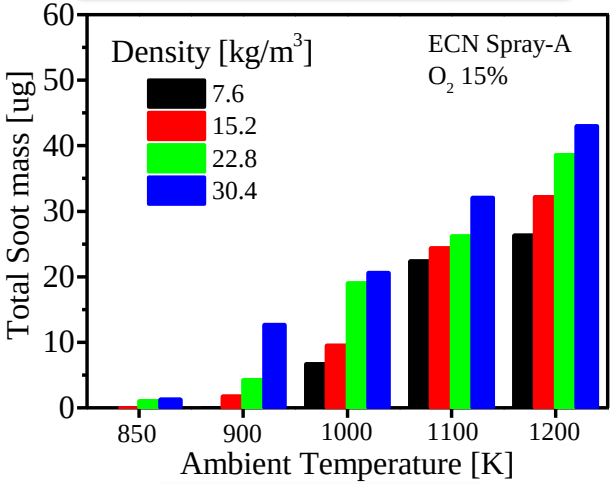

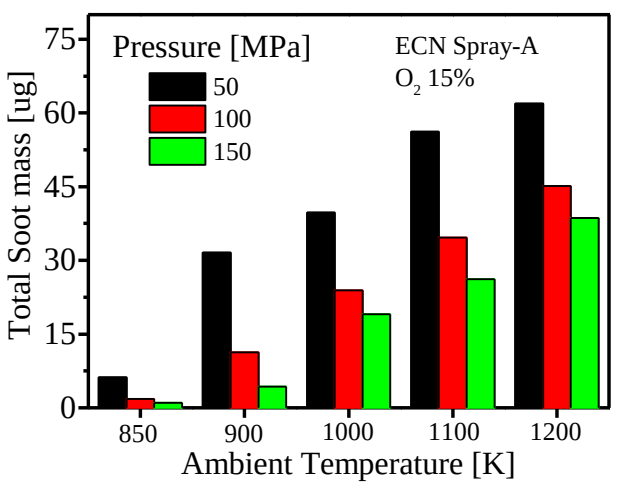

Lift-off length

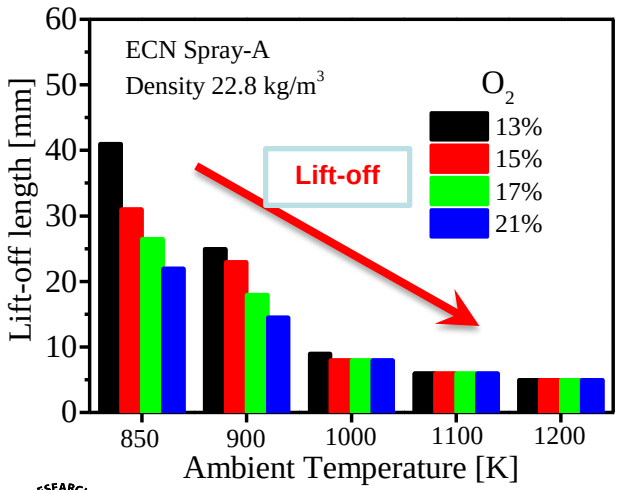

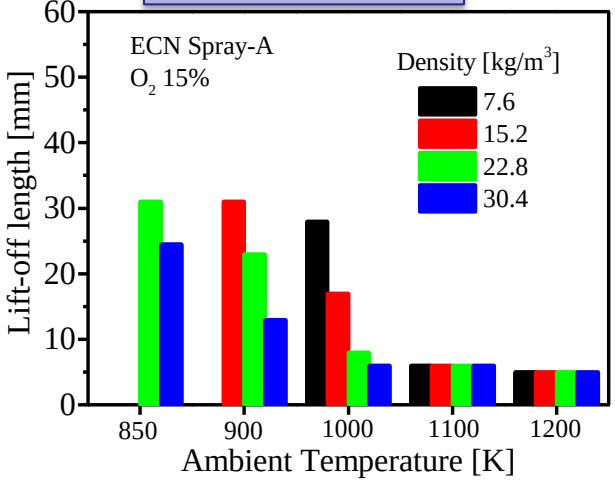

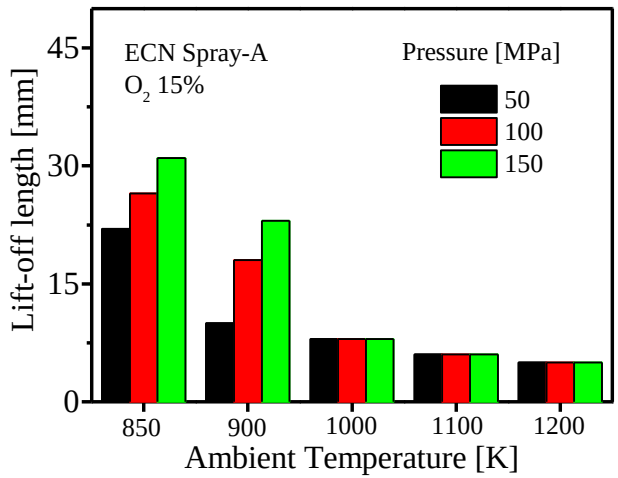

Wang, 2014

Reacting conditions - Soot formation & model sensitivity

C_2H_2 surface growth $C(s) + C_2H_2 \xrightarrow{\omega_2} 3C(s) + H_2$

Soot particle coagulation $nC(s) \xrightarrow{\omega_3} C(s)_n$

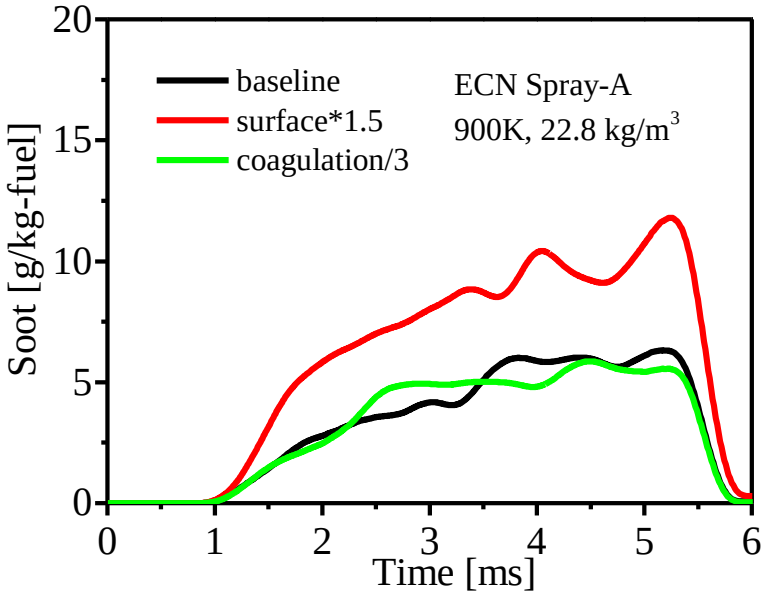

- C_2H_2 assisted surface growth process is the most important process that affects the soot emission, followed by OH oxidation process;
- The surface growth process and the coagulation process affect the soot particle size;

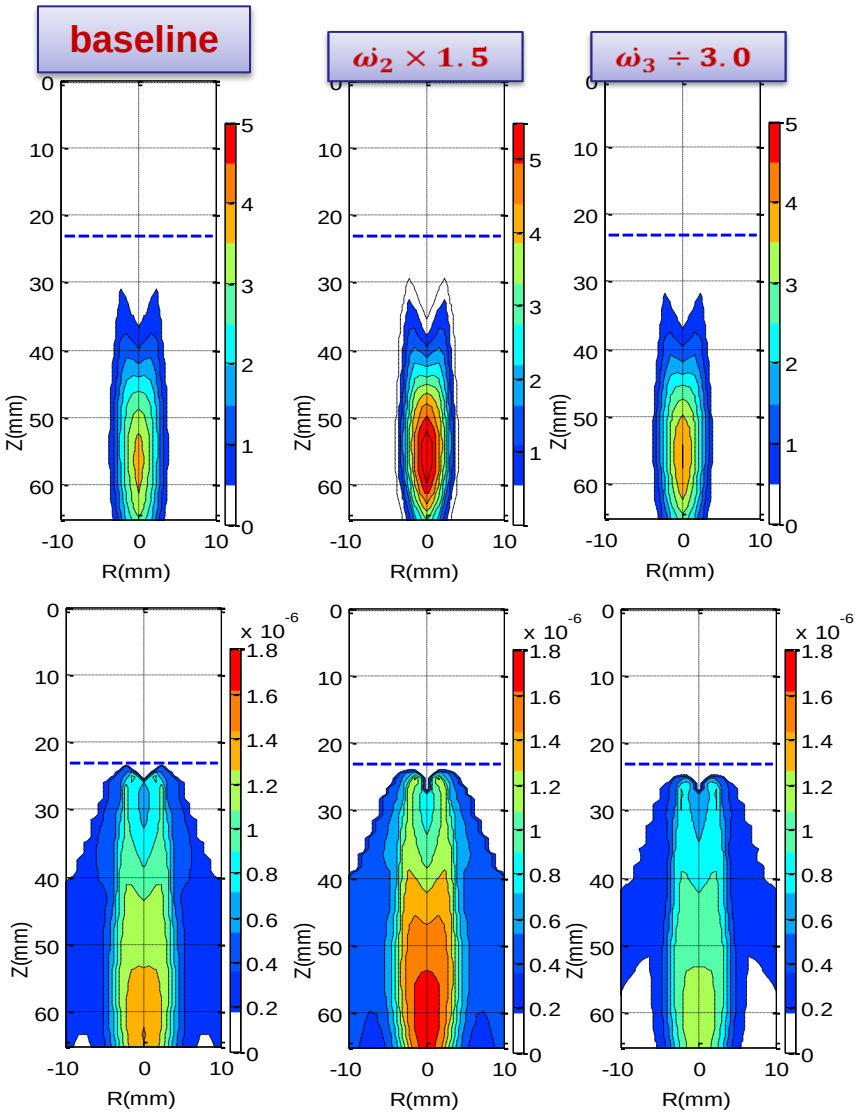

Wang, 2010

Validation – Cummins-Sandia optical engine

	Case A (Early Injection, Low Temperature)	**Case B** (Late Injection, Low Temperature)	**Case C** (Long Ignition Delay, High Temperature)
IMEP [bar]	3.9	4.1	4.5
Injection Pressure [bar]	1600	1600	1200
SOI [deg ATDC]	-22	0	-5
Injection Quantity [mg]	56	56	61
DOI [deg]	7	7	10
Peak Temperature	2200 K	2200 K	2700 K
O2 Concentration [Vol %]	12.7 (with EGR)	12.7 (with EGR)	21 (without EGR)

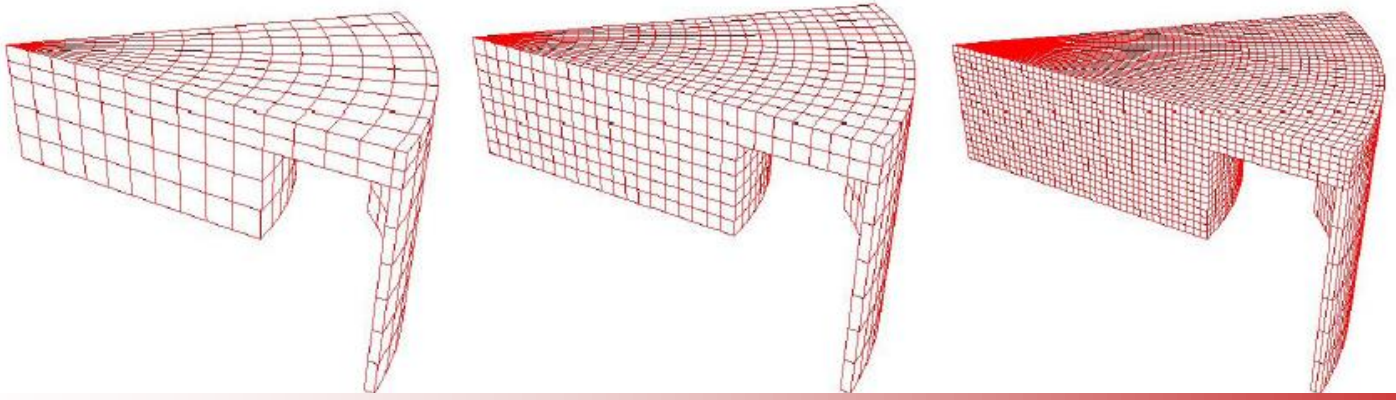

Wang, 2010

Singh, 2007

Liquid and vapor fuel penetration

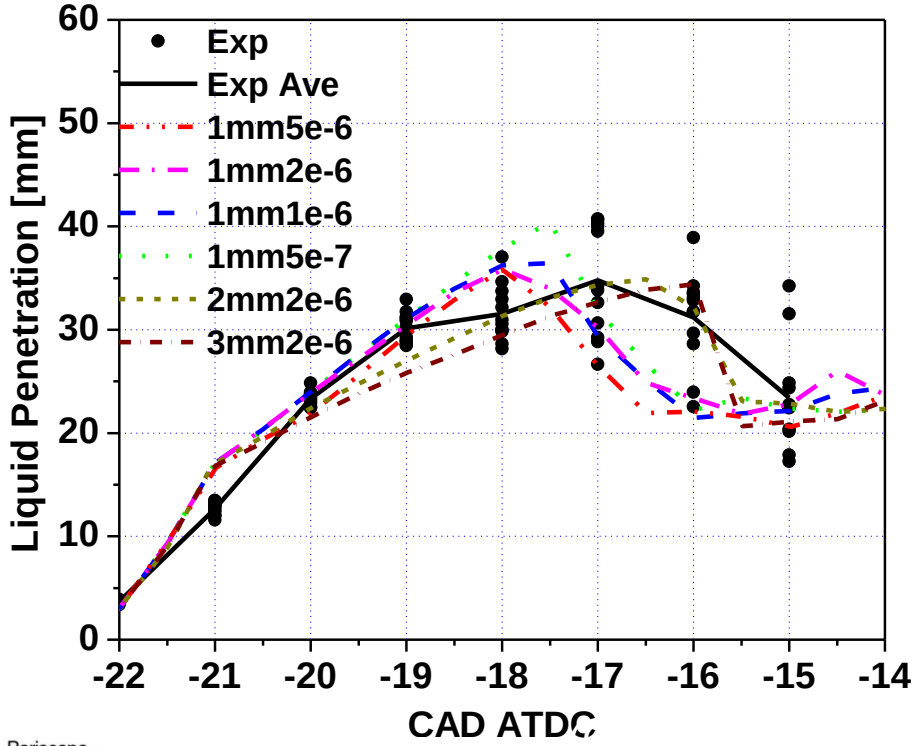

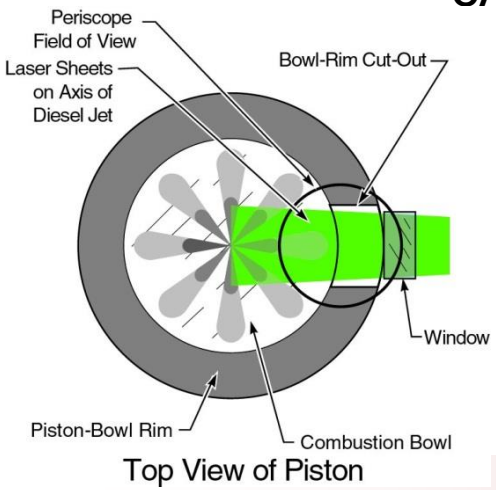

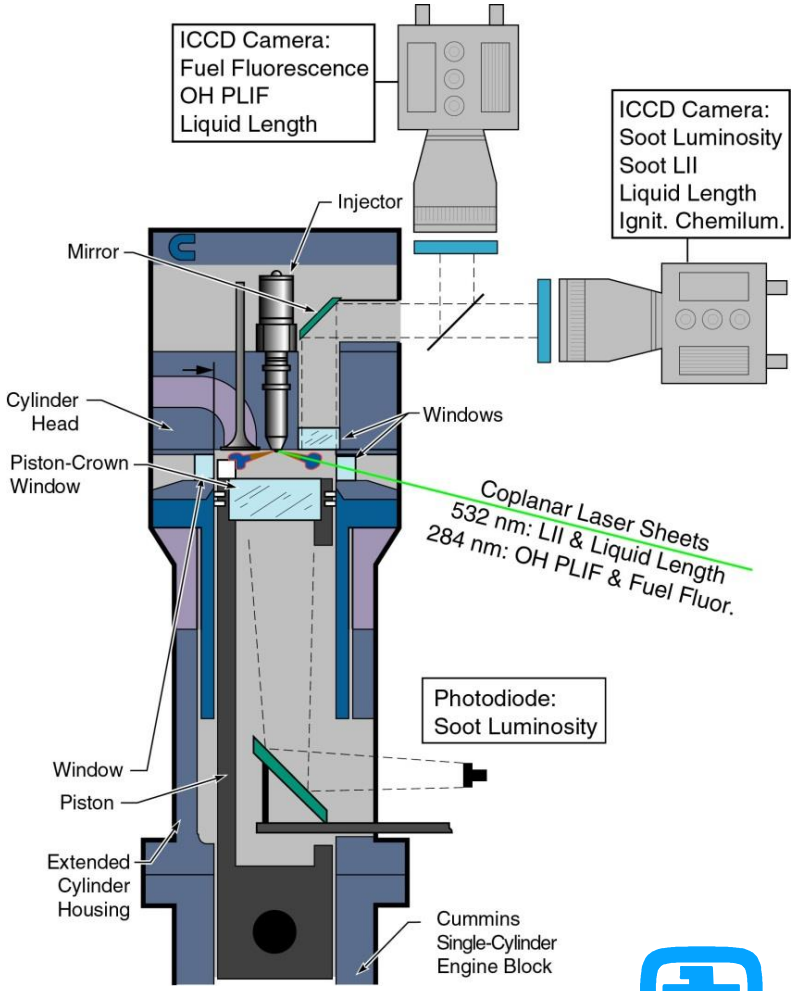

Singh, 2007

Summary

Extensively validated spray models accurately capture the physics of vaporizing sprays under engine conditions

Realistic fuels with non-ideal vaporization effects can be represented

Improved spray models provide consistent fuel distribution predictions, which is a prerequisite for combustion modeling and engine optimization.

Spray predictions can be independent of mesh size and time step;

Recent experimental and modeling work can be accessed through the Sandia Engine Combustion Network (ECN) http://www.sandia.gov/ecn/